(NASA-CR-3808) NUMERICAL METHODS AND A COMPUTER PROGRAM FOR SUBSONIC AND SUPERSONIC AERODYNAMIC DESIGN AND ANALYSIS OF WINGS WITH ATTAINABLE THRUST CONSIDERATIONS (Kentron International, Inc.) 78 p CSCL 01B H1/01

N87-10829

Unclas 43837

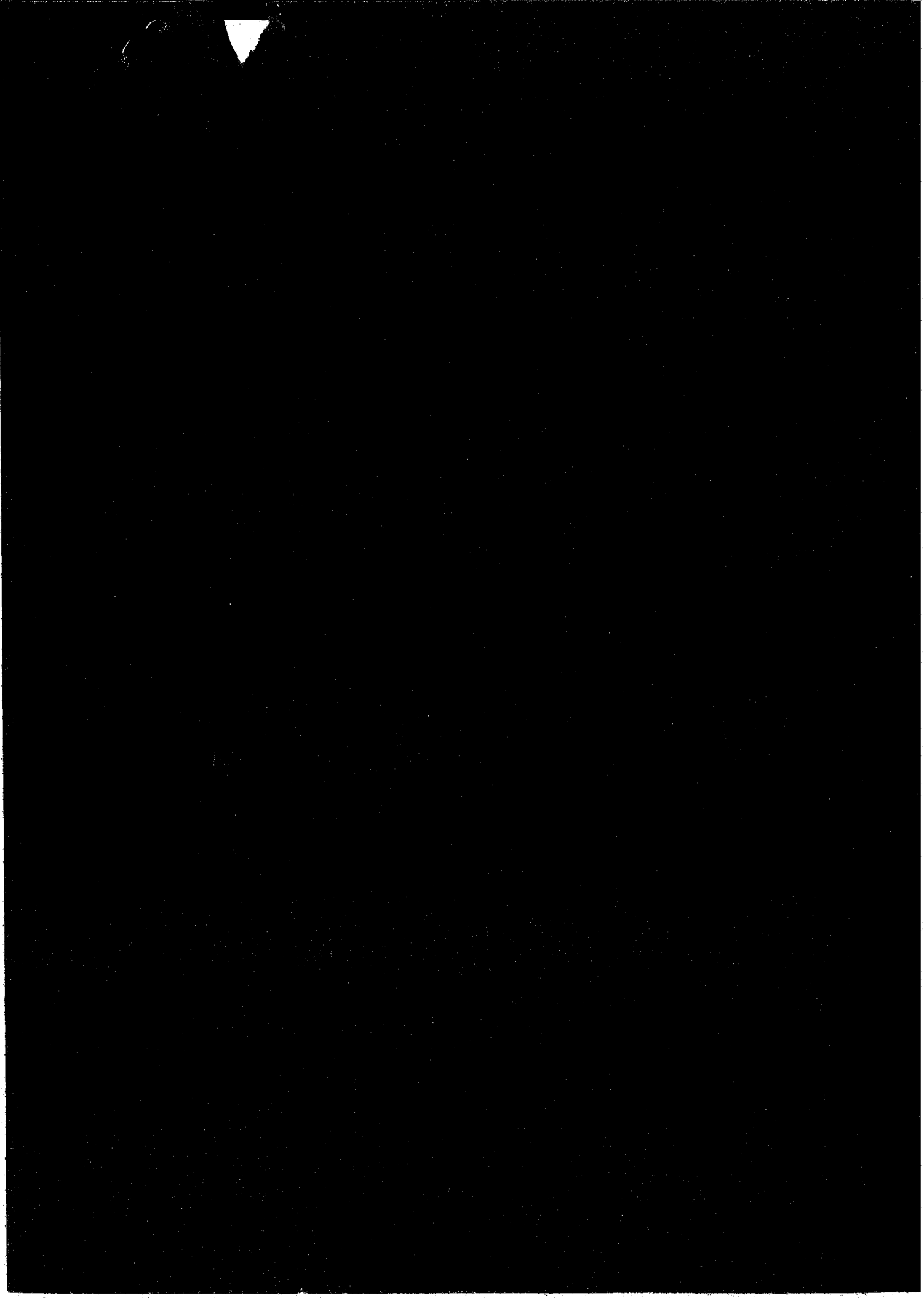

NASA Contractor Report 3808

Numerical Methods and a Computer Program for Subsonic and Supersonic Aerodynamic Design and Analysis of Wings With Attainable Thrust Considerations

Harry W. Carlson and Kenneth B. Walkley
Kentron International Incorporated
Hampton, Virginia

Prepared for
Langley Research Center
under Contract NAS1-16000

National Aeronautics
and Space Administration

**Scientific and Technical
Information Branch**

1984

ABSTRACT

This paper describes methodology and an associated computer program for the design of wing lifting surfaces with attainable thrust taken into consideration. The approach is based on the determination of an optimum combination of a series of candidate surfaces rather than the more commonly used candidate loadings. Special leading-edge surfaces are selected to provide distributed leading-edge thrust forces which compensate for any failure to achieve the full theoretical leading-edge thrust, and a second series of general candidate surfaces is selected to minimize drag subject to constraints on the lift coefficient and, if desired, on the pitching moment coefficient. A primary purpose of this design approach is the introduction of attainable leading-edge thrust considerations so that relatively mild camber surfaces may be employed in the achievement of aerodynamic efficiencies comparable to those attainable if full theoretical leading-edge thrust could be achieved. The program provides an analysis as well as a design capability and is applicable to both subsonic and supersonic flow.

SUMMARY

This paper describes methodology and an associated computer program for the design of wing lifting surfaces with attainable thrust taken into consideration. The approach is based on the determination of an optimum combination of a series of candidate surfaces rather than the more commonly used candidate loadings. Special leading-edge surfaces are selected to provide distributed leading-edge thrust forces which compensate for any failure to achieve the full theoretical leading-edge thrust, and a second series of general candidate surfaces is selected to minimize drag subject to constraints on the lift coefficient and, if desired, on the pitching moment coefficient. A primary purpose of this design approach is the introduction of attainable leading-edge thrust considerations so that relatively mild camber surfaces may be employed in the achievement of aerodynamic efficiencies comparable to those attainable if full theoretical leading-edge thrust could be achieved. The program provides an analysis as well as a design capability and is applicable to both subsonic and supersonic flow.

INTRODUCTION

The aerodynamic performance of wings at subsonic speeds is critically dependent on the amount of leading-edge thrust that can actually be realized. At supersonic speeds, leading-edge thrust plays a reduced role but is not generally negligible. In reference 1, a study of the factors which place limits on the theoretical leading-edge thrust was made, and an empirical method for estimation of attainable thrust was developed. A discussion of the way that attainable thrust considerations affect the selection of low-speed flap systems was given in reference 2. Those design notes have now served as the basis of a system for the design of wing camber surfaces with attainable thrust taken into account.

Consideration of attainable thrust necessitated a design process which operates on the principle of defining an optimum combination of candidate surfaces rather than that of the more generally available design methods which select an optimum combination of candidate loadings or which assign chordwise and spanwise loading distributions. Techniques for the design of supersonic wings using a set of candidate surfaces were introduced in reference 3. However, because that study did not consider leading-edge thrust, only the general approach of that report—the use of surfaces rather than loadings—was applicable to the problem at hand.

In addition to the opportunity to introduce attainable thrust considerations, there are several other advantages associated with the optimum combination of surfaces approach. Because the candidate surfaces may be restricted to individually smooth surfaces, the resultant optimized surface can be free of irregularities due to numerical instabilities. The candidate surfaces may also be chosen to place realistic and practical restraints on camber surface severity, and thus the singularities in surface slope that often arise in optimum loading methods may be eliminated. For special purposes, the optimization may be carried out only on designated portions of the wing such as leading- and trailing-edge areas; a capability particularly useful in design of mission-adaptive wing surfaces.

The methodology and the associated computer program described in this report provide both a design and analysis capability for supersonic as well as subsonic speeds. The subsonic analysis method employed in this program is fundamentally the same as that described in reference 4 and elaborated upon in

reference 2. The basic features of the supersonic analysis are as described in reference 5. A method similar to that of reference 6 has been added to provide for estimation of theoretical leading-edge thrust at supersonic speeds. Methods of estimating attainable thrust for both speed regimes are based on the analysis given in reference 1. The design method, which is applicable to both subsonic and supersonic speeds, is based on the use of Lagrange's method of undetermined multipliers in selecting a combination of candidate surface shapes (and their corresponding loadings) to yield a minimum drag subject to restraints on lift and moment.

Because the analysis methods differ only in minor detail from methods for which extensive correlations of program data and experimental data have been given (see references 1 and 4 for some examples) further demonstrations of applicability will not be given here. However, the design features of the present program, which are new, will be illustrated by means of several sample problems. In some cases, results given by this program will be compared with results of other theoretical design methods.

SYMBOLS

A	candidate surface weighting factor
AR	wing aspect ratio, b^2/S
b	wing span
c	local wing chord
$\bar{c}$	mean aerodynamic chord
c_e	element chord at element midspan
c_{le}	local chord of leading-edge surface
c_r	wing root chord
c_{te}	local chord of trailing-edge surface
C_A	wing axial or chord force coefficient
C_D	wing drag coefficient
ΔC_D	drag due to lift coefficient, $C_D - C_{D,\alpha=0}$ for the same wing with no camber or twist
C_L	wing lift coefficient
$C_{L,des}$	wing design lift coefficient
$C_{L,opt}$	optimum lift coefficient, lift coefficient corresponding to the maximum value of the suction parameter
$C_{L,\alpha}$	wing lift coefficient slope at $\alpha=0$, per degree
C_M	wing pitching moment coefficient
$C_{M,des}$	wing design pitching moment coefficient
C_N	wing normal force coefficient
C_p	pressure coefficient
$C_{p,o}$	pressure coefficient at specified initial point
C_t	section theoretical leading-edge thrust coefficient
e_x	exponent of x used in definition of candidate camber surfaces
e_y	exponent of y used in definition of candidate camber surfaces
i	index of wing element longitudinal position within the program grid system and index used in identification of candidate surfaces

j	index of wing element lateral position within the program grid system and index used in identification of candidate surfaces
k	constant of proportionality
M	Mach number
r	wing section leading-edge radius
R	Reynolds number
S	wing reference area
S_s	suction parameter, $\dfrac{C_L \tan (C_L/C_{L,\alpha}) - \Delta C_D}{C_L \tan (C_L/C_{L,\alpha}) - C_L^2/(\pi AR)}$
t	wing section maximum thickness
x,y,z	Cartesian coordinates
x'	distance in the x direction measured from the wing leading edge
x'_1, x'_2	x' values at front and rear of wing elements
x'_o	x' value of specified initial point
α	wing angle of attack
α_{des}	design angle of attack, corresponding to the design lift coefficient
α_{zt}	wing angle of attack giving a local theoretical leading-edge thrust of zero for a specified wing spanwise station
$\Delta\alpha_{ft}$	range of angle of attack for full theoretical thrust
β	$\sqrt{M^2 - 1}$ for $M > 1$, $\sqrt{1 - M^2}$ for $M < 1$
δ_L	leading edge flap streamwise deflection angle, degrees, positive with leading edge down
δ_T	trailing-edge flap streamwise deflection angle, degrees, positive with trailing edge down
δ_L factor	leading-edge flap deflection multiplier
δ_T factor	trailing-edge flap deflection multiplier
η	location of maximum wing section thickness as a fraction of the chord

λ_N, λ_M	Lagrange multipliers
Λ	wing leading-edge sweep angle

Subscripts

adj	adjusted
ave	average
corr	corrected
des	design
eval	evaluated
goal	goal
le	leading edge
opt	optimum
pre	previous
prog	program
te	trailing edge
vor	vortex

ANALYSIS METHODS

The numerical methods employed in the present computer program for evaluation of the aerodynamic characteristics of specified wing surfaces have, for the most part, been adapted from previously reported work. In the following discussion of the analysis methods, only brief descriptions will be given for portions of the present analysis system which are adequately treated in the references. Significant departures from previously documented methods will be covered in detail.

Basic Loadings at Subsonic Speeds

The development of the basic subsonic analysis computational system is covered in considerable detail in reference 4. That report describes numerical methods which have been incorporated into a computer program to permit the analysis of twisted and cambered wings of arbitrary planform. The computational system is based on a linearized theory lifting surface solution which provides a spanwise distribution of theoretical leading-edge thrust in addition to the surface distribution of perturbation velocities. In contrast to the commonly accepted practice of obtaining linearized theory results by simultaneous solution of a large set of equations, a solution by iteration is employed. The method also features a superposition of independent solutions for a cambered and twisted wing and a flat wing of the same planform to provide, at little additional expense, results for a large number of angles of attack or lift coefficients. A key feature of the superposition technique is the use of leading-edge thrust singularity parameters to identify and separate singular and nonsingular velocity distributions. This separation permits more accurate determination of leading-edge thrust and more accurate integration of pressure distributions for twisted and cambered wings of arbitrary planform. For use in the design mode of the present program, the analysis capability has been expanded so that as many as 44 candidate camber surfaces including the flat surface may be treated simultaneously. Because of the need for evaluation of up to 44 surfaces instead of only two as in reference 4, the maximum number of elements representing the entire wing has been reduced from 4,000 to 1,000, and the maximum number of span stations has been reduced from 41 to 30. Although this change does reduce the possibilities for accurate representation of complex surfaces, the penalties are not as severe as might

be anticipated because it was seldom necessary to use the full capacity of the original program. An example of an array of swept elements used to represent a wing in the numerical solution is shown in figure 1. This representation of a wing in subsonic flow may be compared with the rectangular element representation for supersonic speeds to be shown later.

Basic Loadings at Supersonic Speeds

The basic computation system for supersonic speeds is nearly identical to the method presented in reference 3. That method uses a numerical solution of linearized theory to provide an aerodynamic analysis of twisted and cambered wings of arbitrary planform. Because of the supersonic flow condition, a simple aft marching solution is employed, and no iteration is necessary. This simple solution, however, also requires that only rectangular elements be considered. This in turn creates a tendency toward a solution with oscillations in local velocities. A newly devised means of correcting for these oscillations will be discussed subsequently. Except for this addition and the addition of theoretical leading edge thrust calculations, the only significant change is an alteration of the wing element grid system to eliminate the spanwise row of elements straddling the root chord so as to present a geometry consistent with that of the subsonic analysis. Because of the need to evaluate a large number of surfaces, the maximum number of elements and span stations have been set to the same values used in the subsonic analysis. An example of an array of rectangular elements used to represent a wing in supersonic flow is shown in figure 2. Of course, in practice many more elements would be employed.

Generally, the numerical method used for the evaluation of supersonic linearized theory gives rather smooth distributions of the lifting pressure coefficient as evidenced by the numerous comparisons of numerical method results with exact linearized theory given in reference 5. But for very highly swept leading edges there is a tendency for the formation of oscillations in flat wing pressure distributions. These oscillations center on the correct solution, and thus create no large problems in the determination of overall wing forces and moments. Nevertheless, it is desirable to find a means of suppressing or smoothing these oscillations which for very highly swept wings can become large. An exploration of the causes of

the oscillations and the development of a new smoothing strategy is described in the following paragraphs.

An example of extreme lifting pressure coefficient oscillations given by the basic supersonic analysis system is shown in sketch (a). The data shown here are for a 75° swept leading edge delta wing at a Mach number of 1.41 ($\beta \cot \Lambda = 0.27$) . The parameter $C_p \sqrt{x'/y}$, derived from theoretical distributions of pressure loadings on flat delta wings, permits inclusion of data for several adjacent spanwise stations near the mid-semispan, and compensates for the $1/\sqrt{x'}$ decline in pressure aft of the leading-edge singularity. This and similar plots for other sweep angles and Mach numbers show a wave length of the oscillations which correlates well with the parameter $(\tan\Lambda)/\beta+1$. As shown in sketch (b), the program array of rectangular elements for two adjacent spanwise stations dictates such a pattern. Because of the rectangular element structure, and the nature of supersonic flow, any influence of the outboard span station on the inboard station will be delayed to the chordwise position shown.

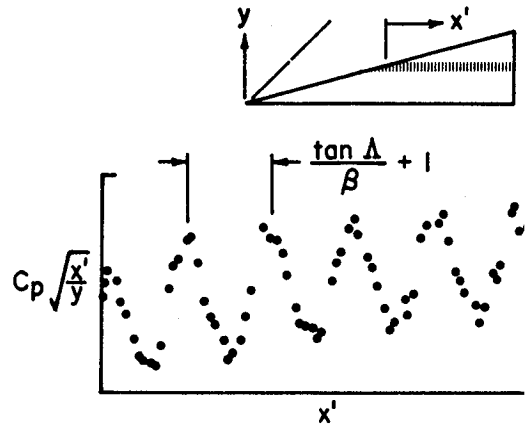

Sketch (a)

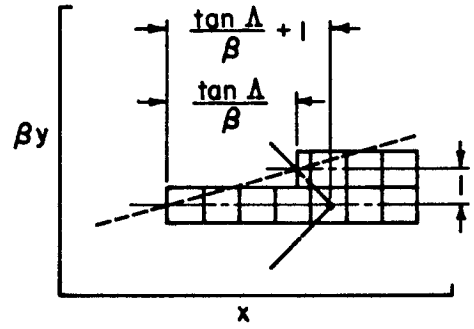

Sketch (b)

The preceding considerations suggest a fairing which covers a number of elements equal to the absolute value of the local parameter, $(\tan\Lambda)/\beta + 1$, and which takes into account the nature of supersonic pressure distributions. This can be accomplished by a least-squares curve fit of one of the

pressure variation forms illustrated in sketch (c). Each of these curves pass through an initial point (x'_o , $C_{p,o}$) and the least squares solution is used to determine the factor k giving the best fit. In the program, a solution is found for each of the forms and the form giving the smallest value for the sum of the squares of the errors is selected. The process begins with the C_p of the first element behind the leading edge. After application of the curve fit, the point immediately behind the initial point is given a new value defined by the k factor of the selected form. Then the process is repeated as often as necessary by advancing one element rearward and by using the just replaced value as a new initial point. In the region of the trailing edge, when the remaining points are less than the defined number, new values are found for all the points.

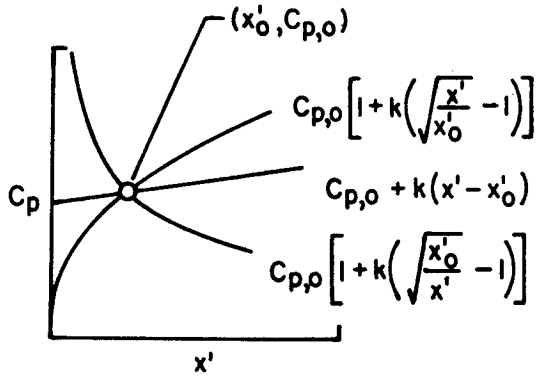

Sketch (c)

Sketch (d) shows the C_p distribution with and without smoothing at the mid-semispan of the example 75° delta wing at M = 1.41. Some irregularities remain, but they are minor compared to the original large oscillations.

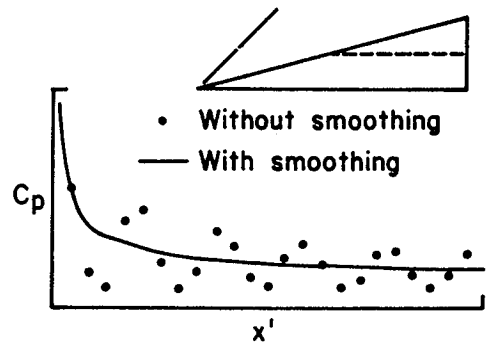

Sketch (d)

A means of extending the basic supersonic computational system to permit calculation of theoretical leading-edge thrust at supersonic speeds was advanced in reference 6. A somewhat simplified system based on the same principles is used in the present computer program. The difference lies in the error analysis and the derivation of an empirical function providing for correction of pressure coefficient locations which was covered in the appendix of reference 6. In the present method, the correction function covers only the first element behind the leading edge instead of the first three. This correction provides the original initial point for the previously described smoothing process which is applied to all other

elements. For these aft elements, the pressure coefficient rather than its location is adjusted.

Figure 3(a) shows the ratio of program C_p to theoretical C_p for leading-edge elements of a series of flat delta wings with different values of the leading-edge sweep parameter, $\beta\cot\Lambda$. The data cover all program span positions up to the maximum permissible for a given $\beta\cot\Lambda$ value. The program pressures are assumed to act at the element quarter chord and the ratios are plotted as a function of the element chord. Most of the observed scatter of the data is due to inclusion of inboard span stations where a stable numerical solution has not yet developed. For these leading-edge elements a curve expressed by the equation:

$$F(x') = \frac{C_{p,\ prog}}{C_{p,\ theory}} = \frac{1 - \left[1 - \sqrt{c_e}\right]^{1.4}}{\sqrt{2\beta\cot\Lambda}}$$

was found to adequately represent the program errors. Figure 3(b) shows the same data in a form which allows the curve fit to be shown as a single line and the program results as a data band. In accordance with the methodology of reference 6, the corrected pressure coefficient location for leading-edge elements is:

$$x'_{corr} = \frac{c_e}{4[F(x')]^2}$$

As pointed out in reference 6, the correction is made to the location rather than to the pressure itself, because a shift in location will correct flat wing data but will not introduce appreciable errors in data for surfaces with pure camber loadings. The remainder of the theoretical leading-edge thrust calculation is performed exactly as described in reference 6, except that the number of elements used in the least squares curve fit to determine singularity strength is governed by the local $(\tan\Lambda)/\beta + 1$ parameter used in the smoothing process.

The pressure distribution smoothing and the leading-edge thrust calculation are seen to be closely related. The corrected C_p location for leading-edge elements is found first, followed by the smoothing process and

the calculation of theoretical leading-edge thrust using the smoothed C_p data.

Attainable Thrust and Vortex Forces

In reference 1, a study of the factors which place limits on the theoretical thrust was made, and an empirical method for estimating attainable thrust was developed. The method is based on the use of simple sweep theory to permit a two-dimensional analysis, the use of theoretical airfoil computer programs to define thrust dependence on local geometric characteristics, and the examination of experimental two-dimensional airfoil data to define limitations imposed by local Mach numbers and Reynolds numbers. In reference 2 the method was modified to give more accurate results at very low Mach numbers. That modified method is employed in the present computer program for the estimation of attainable leading-edge thrust at both subsonic and supersonic speeds.

The computer program described in reference 2 provided three options for the estimation of the magnitude and distribution of forces generated by detached leading-edge vortices which are assumed to form when there is a failure to achieve full theoretical leading-edge thrust. These options are retained in the present program, and may be employed for both subsonic and supersonic speeds. For the reader's convenience, those three options are outlined here.

Option 0. (Default). With this option the vortex force is assumed to act perpendicular to the wing reference plane at the wing leading edge and thus offers no contribution to the wing axial force. This option is used as the program default because it is the most general; it will not be an appropriate option for all program applications.

Option 1. For delta wings and delta wing derivatives, the vortex force center may be located through use of an empirical relationship

$$\frac{y_{vor}}{x \cot\Lambda} = \frac{1}{1 + \sqrt{\tan \alpha}}$$

which as discussed in reference 2 should be applicable to a range of sweep angles from about 50 degrees to about 80 degrees. As shown in sketch (e), it may be possible to provide an approximate location of the center of the vortex pressure field even for wings with significant departures from the delta planform, and for wings which may employ twist and camber or deflected flaps. This may be accomplished by use of the equations:

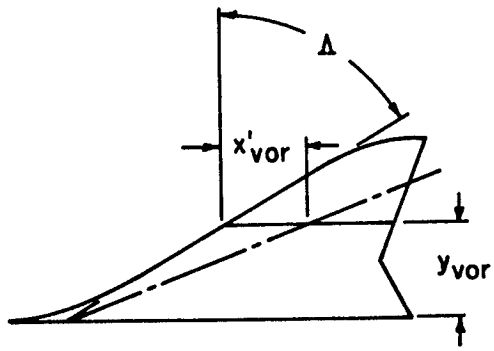

Sketch (e)

$$x'_{vor} = 0.0 \qquad (\alpha_{zt}-\Delta\alpha_{ft}) < \alpha < (\alpha_{zt}+\Delta\alpha_{ft})$$

$$x'_{vor} = \frac{y}{\cot\Lambda}\sqrt{\tan(\alpha-\alpha_{zt}-\Delta\alpha_{ft})} \qquad \alpha > (\alpha_{zt}+\Delta\alpha_{ft})$$

$$x'_{vor} = \frac{y}{\cot\Lambda}\sqrt{\tan(\alpha_{zt}-\Delta\alpha_{ft}-\alpha)} \qquad \alpha < (\alpha_{zt}-\Delta\alpha_{ft})$$

in which Λ is the local leading-edge sweep angle, α_{zt} is the wing angle of attack for local leading-edge thrust of zero, and $\Delta\alpha_{ft}$ is the range of angle of attack for full thrust. This formulation locates the vortex center aft of the leading edge only when full thrust is not realized. However, it does not account for the initiation of leading-edge separation at points along the leading edge other than the apex of the superimposed delta wing.

Option 2. An alternate and very simple means of locating the vortex force center is given by Lan in reference 7. When applied to the present numerical method the location of the vortex force center is:

$$x'_{vor} = c_t c_{ave}\sqrt{\tan\Lambda^2+1}.$$

For options 1 and 2, the distribution of the vortex force is assumed to take the form shown in sketch (f). Since the surface may be cambered, there will be contributions to axial force as well as normal force. If the vortex center lies aft of the local chord midpoint, part of the vortex force will not affect the wing and will be lost.

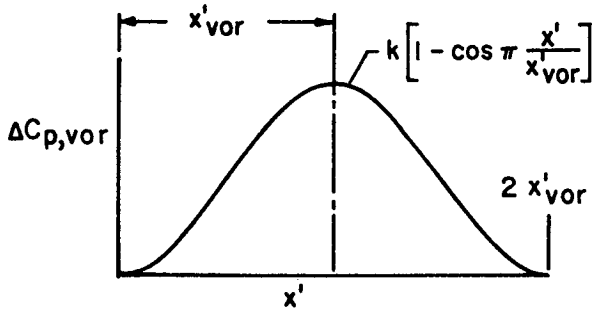

Sketch (f)

Only limited information regarding the selection of the vortex options is available at this time. The default option, with the vortex force acting perpendicular to the wing reference plane at the wing leading edge, was used in the correlations with experimental data given in reference 4. At large angles of attack, that approach seemed to overestimate the vortex effect-probably because much of the vortex field was actually aft of the wing surface rather than at the leading edge. The correlations with experimental data given in reference 2 were made using the vortex location option (1). Generally this produced better results for the examples treated there, however, as pointed out previously, this option is appropriate only for highly swept wings with delta or modified delta planforms. Option 2, from reference 7, is applicable only to wings with sharp leading edges but applies to wings of any planform.

As will be discussed in a later section of this report, it may be desirable for design purposes to know how much a local leading-edge deflection angle may be changed from the local flow alignment condition (presumed to be defined by α_{zt}) and still retain attached flow and full theoretical thrust. This angle of attack range, $\Delta\alpha_{ft}$, may be found by the method described in reference 2.

Force and Moment Coefficients

Aerodynamic coefficients are found by use of integration techniques discussed in reference 4. As discussed in that reference, the wing angle of attack for zero thrust is used to separate the perturbation velocity distribution into two parts, one with a leading edge singularity and one

without. The section normal force is found by a summation of the contributions of individual wing elements for a given spanwise station. Within an individual element, the pressure distribution is assumed to be composed of flat wing and pure camber contributions that depend on the local angle of attack for zero thrust and, for supersonic speeds, also on the relationship between the Mach line and the leading-edge sweep. Within the limits of the element, the pressure distribution will have a segment of one of the forms depicted in figure 4, with the constant k defined so as to pass the curve through the C_p value at the element quarter chord (or the corrected location). A sample curve for the flat wing component at subsonic speeds is shown in sketch (g).

The individual element contributions to the section normal force coefficient are found by use of analytic integration techniques which for subsonic speeds are identical to those given in reference 4 and for supersonic speeds are derived in a similar fashion. Section axial force coefficients are found by summation of the product of the normal force and surface slope dz/dx within individual elements.

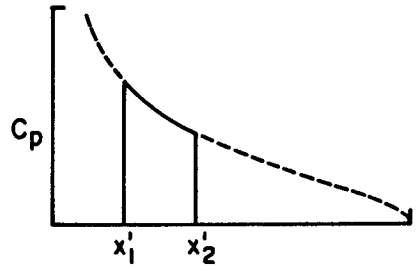

Sketch (g)

DESIGN METHOD

The design method employed in the computer program is directly dependent on the previously discussed analysis methods which are applied to a series of candidate wing surfaces. Leading-edge flow condition considerations in combination with drag minimization techniques are used to find an optimum combination of those surfaces. Inclusion of the influence of attainable thrust on the design dictates that the solution be found by an iterative process.

The process is begun with the evaluation of the aerodynamic characteristics of a program input surface. Except for special design purposes to be discussed later, that surface will be flat. The important design information supplied by this evaluation includes the angle of attack at which the design lift is achieved and spanwise distributions of the angle of

attack for zero thrust and the range of angle of attack for full thrust. This information is used to tailor the wing surface in the leading-edge region to provide distributed leading-edge thrust forces which compensate for any failure to achieve the full theoretical leading-edge thrust. Because this change in the wing surface will change the overall wing lift coefficient at the design condition, it is then necessary to introduce additional incremental wing surfaces to restore the design lift coefficient. The Lagrange method of undetermined multipliers is used to find a combination of additional surfaces which will produce the necessary lift increment with a minimum axial force coefficient. The tailoring of the leading edge plus the combination of additional surfaces will define a new wing surface whose aerodynamic characteristics may be determined by reapplication of evaluation methods. The new surface will generally have a different angle of attack for the design lift coefficient and a different distribution of the angle of attack for zero thrust, necessitating a revised tailoring of the leading-edge surface and a revised definition of the additional surfaces. Thus a solution by iteration is required. The following discussions will elaborate on the steps taken in this process.

Candidate Surfaces

To provide data for use in the optimization process, the evaluation methods are applied to a series of candidate surfaces to evaluate normal force, axial force, and pitching moment coefficients and interference axial force coefficients as well. The candidate surfaces are:

Type	Number	Defining Equation	
Input	1	z defined by table of coordinates	
Flat	2	$z = -\tan 1^{o}\ x'$	
General camber surfaces	3	$z = k\ y^{e_{y,1}(x')}\ ^{e_{x,1}}$	
	4	$z = k\ y^{e_{y,2}(x')}\ ^{e_{x,1}}$	
	5	$z = k\ y^{e_{y,3}(x')}\ ^{e_{x,1}}$	
	6	$z = k\ y^{e_{y,4}(x')}\ ^{e_{x,1}}$	
	7	$z = k\ y^{e_{y,1}(x')}\ ^{e_{x,2}}$	
	8	$z = k\ y^{e_{y,2}(x')}\ ^{e_{x,2}}$	
	9	$z = k\ y^{e_{y,3}(x')}\ ^{e_{x,2}}$	
	10	$z = k\ y^{e_{y,4}(x')}\ ^{e_{x,2}}$	
Trailing-edge camber surfaces	11	$z = k\ y^{e_{y,1}(x'-c+c_{te})}\ ^{e_{x',te}}$	
	12	$z = k\ y^{e_{y,2}(x'-c+c_{te})}\ ^{e_{x,te}}$	
	13	$z = k\ y^{e_{y,3}(x'-c+c_{te})}\ ^{e_{x,te}}$	
	14	$z = k\ y^{e_{y,4}(x'-c+c_{te})}\ ^{e_{x,te}}$	
Leading-edge camber surfaces	15	$z = \tan 1^{o}\ x' \left[1 - \frac{2}{3}\sqrt{\frac{x'}{c_{le}}}\right]$	$0<x'<c_{le}$
	to		
	44	$= \frac{1}{3} \tan 1^{o}\ c_{le}$	$c_{le}<x'$

The first surface is defined by an input TZORD table described in a later section. For special design problems, the user may choose to use such a surface. However, for conventional design purposes, a surface with z = 0 everywhere is preferable and this surface is provided by a program default. The second surface is a flat surface at one degree angle of attack.

Surfaces 3 to 10 affect the entire wing and are called general camber surfaces. The program user may select a desired number of these surfaces from 0 to 8 to be taken in the order listed (for instance, if 4 surfaces are called for, surfaces 3 to 6 will be used). The order can not be changed but other exponents can be substituted for $e_{y,1}$ to $e_{y,4}$ and for $e_{x,1}$ and $e_{x,2}$. The program will use all eight surfaces unless the user chooses otherwise; the program default for the number of general camber surfaces is 8. Typical general camber surfaces for a delta wing with default exponents are illustrated in figure 4.

Surfaces 11 to 14 are intended to cover a wing trailing-edge region for special purposes such as design of mission adaptive surfaces or a "first cut" at selection of trailing-edge flap geometry. If desired, these surfaces can be used as additional general camber surfaces by setting the trailing-edge surface chords equal to the wing chords and selecting an $e_{x,te}$ value different from $e_{x,1}$ and $e_{x,2}$. The user may select a desired number of these surfaces from 0 to 4 to be taken in the order listed. The program default for the number of trailing edge modifying surfaces is 0. Typical trailing-edge surfaces are also illustrated in figure 4.

The remaining surfaces serve the purpose of modifying the wing leading-edge region. They are designed to have a much larger effect on leading-edge surface slope dz/dx than any of the other surfaces (except the flat surface at $\alpha = 1^{\circ}$) and thus to exert a strong influence on the important design factor, the wing angle of attack for a local leading-edge thrust of zero. There is one leading-edge modifying surface for each of the wing spanwise stations from wing root to wing tip. Each of these surfaces has the specified surface ordinates only for a strip one unit wide centered on that particular

station. Everywhere else, the surface has an ordinate of zero. A typical leading-edge modification surface for the third of seven semispan stations for a subsonic design Mach number is shown in sketch (h). For supersonic speeds, the shape would be similar but the leading edge would be unswept.

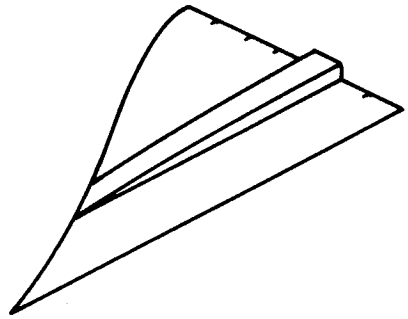

Sketch (h)

Since the optimization process is critically dependent on these leading-edge surfaces, the user has no option for reducing the number. The user may, however, select the area to be affected by the leading-edge modification by entering a tabular schedule of c_{le} versus span station to replace the program default table which sets c_{le} at all span stations equal to the wing root chord. Reduced areas for the leading-edge modification could very well give an optimized wing design with better performance than that given by the conservative program default. However, very small leading-edge modification areas could lead to erroneous results. Section aerodynamic and geometric data at span stations where fewer than 2 or 3 elements cover the chord of a leading-edge modification surface could be suspect. The number of elements in a given chord may be approximated as:

$$N = \frac{c_{le}}{b/2} \text{ JBYMAX ELAR} \qquad \text{(subsonic speeds)}$$

$$N = \frac{c_{le}}{b/2} \frac{\text{JBYMAX}}{\beta} \qquad \text{(supersonic speeds)}$$

with JBYMAX and ELAR as defined in the program description section of this report. Because computational costs tend to increase as the fourth power of JBYMAX and the second power of ELAR, an increase in the element aspect ratio is the more efficient means of providing for increased definition. At supersonic speeds the only recourse is to increase JBYMAX.

Influence of Leading-Edge Conditions on Wing Design

Wing aerodynamic performance is critically dependent on leading-edge flow conditions. If as depicted in sketch (i), the wing section thickness and leading edge radius are large enough to retain attached flow and full leading-edge thrust for a given set of flight conditions there will be little need to depart from a flat lifting surface. If, on the other hand, the wing section is very thin with little or no possibility for the development of leading-edge thrust, comparable aerodynamic performance can be obtained only by shaping the wing camber surface as shown in sketch (j) to distribute the pressures so that as much as possible of the section lifting force is generated on the forward portion of the section where a thrust force can be generated. For wing sections with thickness and radius which are appreciable but not large enough to generate full thrust at the design condition, a compromise may be made by introducing just enough camber to reduce the angle between the upwash vector and the mean camber surface to a value which will permit attached flow. Such an intermediate solution is depicted in sketch (k). As will be discussed subsequently, the attainable thrust prediction method provides the basic information required in a design process which takes advantage of the possibilities for thrust generation to reduce the severity of the design camber surface.

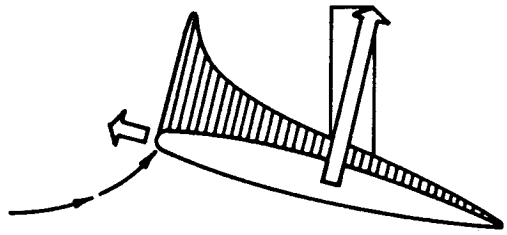

Sketch (i)

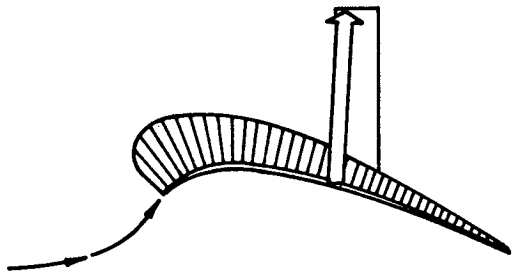

Sketch (j)

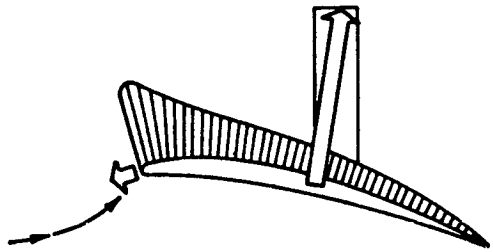

Sketch (k)

Selection of Leading Edge Surfaces

The design process begins with the evaluation of the aerodynamic characteristics of the program input surface. Except for special purpose designs, that surface will be flat (the program default surface), and such a surface will be used for illustrative purposes. The input surface is not allowed to change in the design process, and thus the greatest potential for drag minimization will be permitted with an input surface which places no restraints on the design. Among the information provided by the program evaluation of the input surface is a spanwise distribution of the range of angle of attack for full thrust, which might appear as shown in sketch (l). For angles outside of this range, the attainable thrust levels are less than the full theoretical values. The evaluation of the input surface also provides an estimate of the angle of attack required to generate the design lift coefficient which will be designated the design angle of attack.

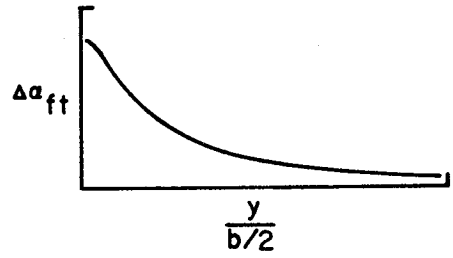

Sketch (l)

The object of the design process is to alter the wing angle of attack for zero thrust distribution to create a relationship between α_{zt}, $\Delta\alpha_{ft}$, and α_{des} similar to that shown in sketch (m) wherein the upper limits of the range of full thrust for the cambered wing are coincident with the design angle of attack. This will give a design with the mildest camber surface capable of an aerodynamic efficiency comparable with the full theoretical leading-edge thrust efficiency.

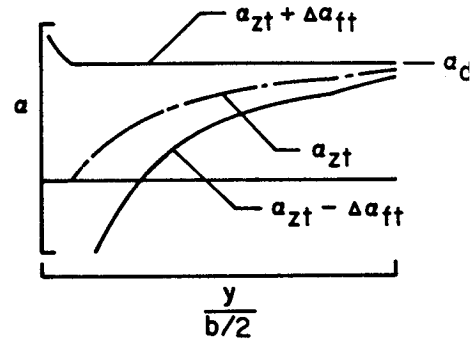

Sketch (m)

The program design is carried out by iteration. For any design iteration, the leading edge surface weighting factors are set equal to $\alpha_{des} - (\alpha_{zt} + \Delta\alpha_{ft})$. For a flat input surface with $\alpha_{zt} = 0^{\circ}$, the leading edge surface weighting factors for the first iteration would be as shown in sketch (n).

The resultant surface defined by the addition of the spanwise distribution of leading-edge surface weighting factors will alter the wing lift and moment coefficient. The optimization procedure, to be described in the next section, is then used to find additional surfaces (general camber surfaces) which restore the wing lift coefficient to the design value and introduce a moment increment to approach the design moment coefficient and do so with the least possible chord force. Because these general camber surfaces have an influence on the spanwise distribution of the angle of attack for zero thrust and the design angle of attack, it is necessary to evaluate these quantities and then find a distribution of incremental leading-edge surface factors to rematch the upper limit of the range of full thrust with the design angle of attack.

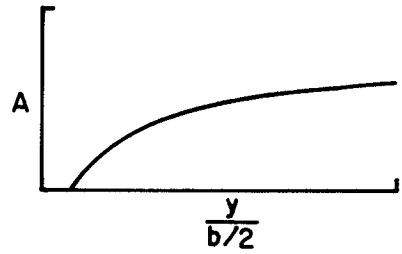

Sketch (n)

Selection of General Camber Surfaces

The Lagrange method of undetermined multipliers is used to define general camber surface weighting factors which minimize the wing axial force while producing a specified increment in normal force coefficient and, if desired, a specified increment in moment coefficient. Application of this method to the problem of selecting an optimum combination of loadings was covered in some detail in reference 5. For the present application, the following set of equations is used to establish the strength of each of the candidate surface factors:

$$\sum_{i=2}^{i=n} C_{A,1i}\, A_i + \lambda_N C_{N,1} + \lambda_m C_{m,1} = 0$$

$$\sum_{i=2}^{i=n} C_{A,2i}\, A_i + \lambda_N C_{N,2} + \lambda_m C_{m,2} = 0$$

$$\vdots \qquad \vdots \qquad \vdots \qquad \vdots$$

$$\sum_{i=2}^{i=n} C_{A,ni}\, A_i + \lambda_N C_{N,n} + \lambda_m C_{m,n} = 0$$

$$\sum_{i=2}^{i=n} C_{N,2}\, A_i + 0 + 0 = -\sum_{i=n+1}^{i=N} C_{N,i}\, A_i$$

$$\sum_{i=2}^{i=n} C_{m,i} A_i + 0 + 0 = C_{m,des} - C_{m,pre} + C_{m,corr} - \sum_{i=n+1}^{i=N} C_{m,i}\, A_i$$

where n = number of general camber surfaces and trailing edge camber surfaces

N = total number of camber surfaces, n + JBYMAX

$C_{m,pre}$ = pitching moment coefficient evaluated in the previous iteration

$C_{m,corr}$ = pitching moment coefficient correction based on differences between anticipated and realized pitching moment coefficients in previous iterations.

If moment coefficient restraints are not to be applied, the terms in the bottom row and the column just left of the equal sign are eliminated. With the surface factors evaluated by standard numerical procedures for solutions of simultaneous equations (up to 15), surface slopes and pressure distributions of the optimized surface are found by linear combination.

Summary of the Design Process

As has been described, the design process is carried out by a cycling through the following steps:

(a) definition of the aerodynamic characteristics of the wing surface including the spanwise distribution of the angle of attack for zero thrust and the design angle of attack

(b) definition of incremental leading edge surface factors to match the upper limit of the range of full thrust with the design angle of attack

(c) definition of general camber surface factors to minimize the wing axial force while maintaining the design lift coefficient and approaching the design pitching moment coefficient.

The iteration is stopped when from one iteration to the next, the design angle of attack changes by less than 0.01 degrees and the design pitching moment coefficient changes by less than 0.001.

Although the program design procedures were developed specifically to take advantage of attainable thrust in an attempt to define mild camber surfaces which yield aerodynamic performance comparable to that attainable with full theoretical thrust, there are other ways in which the program design features can be used. An alternate approach would be to use the attainable thrust information to design a wing with a compromise between aerodynamic performance at two or more design points, for instance at a cruise point and a maneuver point at the same Mach number. One way of working this problem would be to design a sharp leading-edge surface for an intermediate design lift coefficient, and to use a subsequent evaluation with the actual wing thickness and leading-edge radius to give performance estimates for the design points. If attainable thrust at one or both design points is less than the full theoretical value, it may be necessary to find the best compromise by iteration.

Two principal goals of the design approach of this paper, as applied to a sharp leading edge wing, are the alignment of the wing leading edge with the local upwash and the generation of a significant amount of normal force in the vicinity of the leading edge so as to create a distributed thrust to replace

the lost concentrated leading-edge thrust. At first glance, these two goals may appear to be contradictory. The alignment of the leading edge with the local flow will give a loading of zero at the leading edge which, of course, cannot produce the desired thrust. The saving feature of the design concept is the rapid curvature of the surface away from this condition due to the optimized combination of candidate surfaces. This permits the rapid development of thrust producing loadings immediately behind the leading edge. The handling of leading edges in linearized theory has always created problems such as theoretically infinite pressures for flat surfaces, and theoretically infinite slopes for wing design surfaces. However, this is a very localized condition and, except in the immediate vicinity of the singularities, the solutions are reasonable. The failure of numerical methods to reproduce these singularities poses no real handicap and in the design case offers a more practical surface than would an analytic solution.

Evaluation of the Design

Although evaluation methods are used to determine the aerodynamic characteristics of each of the candidate surfaces, the results for the optimized combination of surfaces may not provide a true representation of the aerodynamic efficiency of the wing design in all cases. Because the evaluation data provided in the program design mode is based on the direct addition of surface ordinates and aerodynamic coefficients for up to 44 different candidate surfaces, each of which may introduce numerical calculation errors, there is a possibility of an accumulation of errors.

To provide a better assessment of the aerodynamic characteristics of the just completed design which is consistent with evaluations of other wing surfaces, a special program feature has been provided. If the program user chooses, the many contributing surfaces may be consolidated to provide a single camber surface which in combination with a flat surface at one degree angle of attack will be used in a "standard" evaluation. When this option is exercised, the program will create, through interpolation and extrapolation, a table of camber surface ordinates to replace the original input (or program default) surface, and then perform the normal evaluation procedures beginning with the determination of program geometry information for this new surface.

User Control of the Design

There are a number of ways in which the program user can exert an influence on the design beyond the normal selection of design Mach number, Reynolds number, lift coefficient, and if desired, moment coefficient. As mentioned previously, the user may exercise some control over the candidate surfaces to be used in the design. The use of this capability for special purpose designs will be illustrated in one of the program application examples to be given later.

The user may also affect the design by overriding the distribution of leading-edge surface factors provided by the program. Because these factors are determined by a numerical iteration process, the design may result in a wing surface with irregularities in the spanwise variation of camber surface ordinates. As described in the section entitled "Program Description," the user may substitute a smoothed set of leading-edge surface factors, and redesign the wing to produce a camber surface without irregularities.

The provision for alteration of the distribution of leading-edge surface factors may also be used for another purpose. When aerodynamic data for a camber surface design from the program evaluation mode differs significantly from the data developed in the design mode, there is a possibility that the wing performance may be improved by user control of the leading-edge surface factors. There are two primary ways in which the design as evaluated may differ from the design goals. First, as shown in sketch (o), there may be differences in the spanwise distribution of the angle of attack for zero thrust. This is a measure of the failure to provide the proper relationship between leading-edge surface slope and the local upwash. For reasons discussed previously, the evaluation data must be considered as the more accurate. Any tendency for the design data to underestimate or to overestimate this angle can be compensated for by an adjustment to the leading-edge surface factors used in the design. Also, as shown in

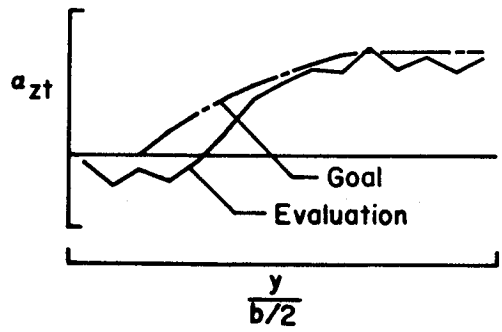

Sketch (o)

sketch (p), the evaluation data may give an optimum lift coefficient that does not correspond to the design lift coefficient. Again the evaluation data must be regarded as the more accurate and again a correction may be made by an adjustment to the leading-edge surface factors. The following equation has been found to provide a revised leading-edge surface factor distribution that offers improved performance in most cases where either or both of the preceding discrepancies are significant.

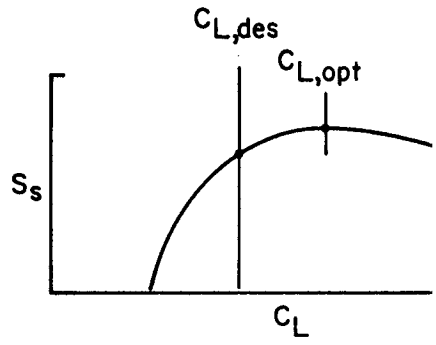

Sketch (p)

$$A_{le,adj} = \frac{C_{L,des}}{C_{L,opt}} \left[\frac{A_{le} \times 1^{o} + \alpha_{zt,goal} - \alpha_{zt,eval}}{1^{o}} \right]$$

For the user's convenience, a listing of the leading-edge factors used in the design and a listing of suggested values which may lead to improved performance are provided.

PROGRAM DESCRIPTION

The computer program entitled "Design and Analysis of Wings with Attainable Thrust Considerations" may be obtained for a fee from:

Computer Sofware Management and
Information Center (COSMIC)
112 Barrow Hall
University of Georgia
Athens, GA 30602
(404) 542-3265

Request the program by the designation LAR-13315. This program is written in FORTRAN IV for use on the Control Data 6600 and Cyber series of computers.

The first record in the input is a program run identification accepting up to 80 characters. The remainder of the input is placed in NAMELIST format under the name INPT1.

The wing planform information is specified by a series of leading-edge and trailing-edge breakpoints. Up to 21 pairs of coordinates may be used to describe the leading edge and up to 21 pairs to describe the trailing edge. The planform input data in program terminology are:

NLEY number of leading-edge breakpoints (limit of 21)

TBLEY table of leading-edge y-values in increasing order of y from wing root to wing tip

TBLEX table of leading-edge x-values corresponding to the TBLEY table

NTEY number of trailing-edge breakpoints (limit of 21)

TBTEY table of trailing-edge y-values in increasing order of y from wing root to wing tip

TBTEX table of trailing-edge x-values corresponding to the TBTEY table

XMAX largest x-ordinate occurring anywhere on the planform

SREF wing reference area for use in aerodynamic force and moment coefficients

CBAR wing reference chord for use in aerodynamic moment coefficients

XMC x-location of moment reference center

ELAR desired element aspect ratio (for flat and mildly cambered wings an element aspect ratio approximately one-half the full wing aspect ratio is recommended, for small chord leading-edge or trailing-edge areas it may be necessary to use a large element aspect ratio to place at least two elements within the chord. The number of elements in a given chord, c_{le} or c_{te}, may be approximated as:

$$N = \frac{c_{le} \text{ or } c_{te}}{b/2} \times \text{JBYMAX} \times \text{ELAR}$$

Because computational costs tend to increase as the fourth power of JBYMAX and the second power of ELAR, an increase in the element aspect ratio is the more efficient means of providing for improved definition. At supersonic speeds, where ELAR is set to $1/\beta$, the only recourse is to increase JBYMAX.

The size of the wing in program dimensions is controlled by the entry:

JBYMAX integer designating the number of elements in the spanwise direction (limit of 30)

The necessary scaling is done within the program by use of a scale factor 2(JBYMAX)/(SPAN x β). The number of complete wing elements N corresponding to a given JBYMAX may be approximated as

$$N = 4 \times JBYMAX^2 \times \frac{ELAR}{\text{wing aspect ratio}}$$

The program has been written to accommodate 500 right hand panel elements. Generally, the JBYMAX integer will be less than the limit of 30. The normal range is 10 to 15 for subsonic speeds and 20 to 30 for supersonic speeds. Computational costs tend to increase as the square of the number of elements.

The wing mean-camber surface may be specified by a set of tabular entries. However, if a flat wing analysis is to be performed or if a flat wing is to be used as the initial surface in a design process, these entries are not required. If a wing surface is input, the section mean-camber surface must be specified by exactly 26 chordwise ordinates at up to 32 span stations. When fewer than 26 camber coordinates are used to define the sections, the ordinate tables must be filled with enough zeros to complete the list of 26. The necessary section information is:

NYC — number of spanwise stations at which chordwise sections are used to define the mean camber surface (limit of 32)

TBYC — table of y values for the camber surface chordwise sections, increasing order of y from root to tip

NPCTC — number of chordwise stations used in mean camber surface definition (limit of 20)

TBPCTC — table of chordwise stations, in percent of chord, at which camber surface ordinates are defined; in increasing order from leading to trailing edge

TZORDC — table of mean camber surface z-ordinates corresponding to the TBPCTC table; the full 26 values for the root chord (including zeros for values in excess of NPCTC) are given first, followed by similar information for all spanwise stations in increasing order of y

The TZORDC table may be multiplied by a scale factor TZSCALE if desired. This may be useful if the original tabulated ordinates are nondimensionalized with

respect to a single measurement (the wing root chord, for example) or if it is desirable to evaluate the effect of change in camber surface severity.

The following wing section information is required for the calculation of attainable leading-edge thrust and leading edge separation forces.

NYR — number of spanwise stations at which airfoil section information is supplied (limit of 21)

TBYR — table of y values for airfoil section information, increasing order of y values from root to tip

TBTOC — table of airfoil maximum thickness as a fraction of the chord, t/c

TBETA — table of the section locations of maximum thickness as a fraction of the chord, η

TBROC — table of the leading-edge radii as a fraction of the chord, r/c

IVOROP — vortex location option

- 0 full vortex force acts normal to wing reference plane of the wing leading edge, does not contribute to axial force, default
- 1 vortex center given by empirical relationships derived from delta wing experimental data
- 2 vortex center given by the method of Lan (ref. 7)

The flight or test conditions are specified as:

XM — free-stream Mach number

RN — free-stream Reynolds number (based on $\bar{c}$) in millions, $R/10^6$

NALPHA — number of angles of attack to be calculated (limit of 19)

TALPHA — table of angles of attack to be calculated, in degrees

The commonly accepted practice of performing subsonic calculations for a Mach number of 0.0 is not appropriate for this program. Realistic estimates of attainable thrust can be made only if both the Mach number and the Reynolds number correspond to actual conditions. In fact, an error message is written when XM = 0.0 is input and execution stops. A Reynolds number of 0.0 may be

input as a convenient means of obtaining sharp leading edge solutions without altering the section geometric data. For use of the program in the design mode, a wide range of angles of attack is required. This range must cover the angle for $C_{L,des}$ of the original and all subsequent surfaces. An error message is written when the angle of attack range is too small.

To determine perturbation velocity distributions for the input camber surface, the flat wing surface at 1^{o} angle of attack, and the candidate camber surfaces used in the design mode, a maximum of 50 iterations are provided. If this number is reached without the convergence criteria being met, the results for the 50^{th} iteration will be printed with an appropriate message. The maximum number of iterations may be changed by the entry:

ITRMAX maximum number of perturbation velocity iterations (default 50)

The program convergence criteria is met when, for all wing surfaces, the average difference in perturbation velocity between successive iterations is less than one-half of one percent (0.005) of the average velocity over the wing. If the average velocity for any of the wing surfaces is less than the average velocity of the flat surface at 1^{o} angle of attack, the flat wing surface value is used instead. In many instances this criteria may be more stringent than necessary. If desired the convergence criteria may be changed by an entry:

CNVGTST perturbation velocity convergence criteria (default 0.005)

The following entries control the solution for the optimized surface in the program design mode. For the analysis of a specified wing surface, omit these entries:

CLDES design lift coefficient (if CLDES is not specified, the program defaults to CLDES = 0.0 which triggers an analysis only solution)

CMDES design pitching moment coefficient (if CMDES is not specified, the program defaults to CMDES = 1000.0 which triggers an optimization solution without moment restraint)

In attempting to meet the convergence criteria for wing design, the program provides for a maximum of 20 iterations. If this number is reached without the convergence criteria being met, the results for the 20^{th} iteration will be printed with a warning of the failure to meet the criteria. If desired, the maximum number of design iterations may be increased or decreased by the entry:

ITRDESM maximum number of design iterations

The user has no control over the design convergence criteria.

The remainder of the design mode entries are optional. These can be very valuable for program user control of the design process but are covered by program defaults if the user chooses not to exercise the options.

NGCS number of general camber surfaces covering the entire wing (limit of 8, program default 8).

To preserve the original surface between the leading-edge modification surfaces and the trailing-edge modification surfaces, NGSC may be set to zero. In this case, user options for both leading-edge and trailing-edge modifications must be employed.

EXPY1, EXPY2, EXPY3, EXPY4 exponents of y used in definition of general camber surfaces (program defaults; EXPY1 = 0.0, EXPY2 = 1.0, EXPY3 = 2.0, EXPY4 = 3.0)

EXPX1, EXPX2 exponents of x' used in definition of general camber surfaces (program defaults; EXPX1 = 1.5, EXPX2 = 2.0)

The following entries control the region of the wing affected by the leading-edge modification surfaces. Because wing aerodynamic performance is critically dependent on the surface shape and pressure loading in the leading edge region, these surfaces are essential to the optimization process. Program defaults provide candidate surfaces which generally will provide a

camber surface design with good aerodynamic efficiency. The program user, however, may want to tailor a camber surface solution more appropriate to the problem at hand and may want to search for solutions offering greater efficiency.

NLEC number of breakpoints used in definition of the area of the wing to be affected by leading-edge modification surfaces (limit of 21, program default 2)

TBLECY table of y values at breakpoints used in definition of the area of the wing to be affected by the leading-edge modification surfaces, in increasing order of y from the wing root to the wing tip (program default 0.0, TBLEY(NLEY))

TBLEC table of c_{le} values corresponding to the TBLECY table (program default TBTEX(1) - TBLEX(1) for both entries)
See note under the ELAR entry regarding the definition of leading-edge areas. It may be necessary to change ELAR or to place limits on non-zero c_{le} values.

The following entries control the region of the wing affected by the trailing-edge modification surfaces and the streamwise section shape of these surfaces. The program defaults exclude these surfaces:

NTES number of trailing-edge modification surfaces (limit of 4)

NTEC number of breakpoints used in definition of the area of the wing affected by trailing-edge modification surfaces (limit of 21)

TBTECY table of y values at breakpoints used in definition of the area of the wing affected by trailing edge modification surfaces, in increasing order of y from the wing root to the wing tip

TBTEC table of c_{te} values corresponding to the TBTECY table
See note under ELAR entry regarding the definition of trailing-edge areas. It may be necessary to change ELAR or to place limits on non-zero c_{te} values

EXPXTE exponent used in definition of the trailing-edge modification surfaces (exponents of y are the same as those used in definition of the general camber surfaces)

The following user option provides a degree of control over the smoothness of the camber surface solution. Program-determined weighting factors for the leading-edge modification surfaces are subject to numerical inaccuracies which may produce z ordinates which do not have a smooth variation with respect to the y dimension. Through use of this option, the user may substitute a smoothed set of leading-edge surface factors for the program tabulated values. With the present program two runs are required; the first to find the non-smoothed values, and the second to operate with the smoothed values.

IAFIX smoothing operation indicator, set IAFIX = 1 if smoothing is to be employed (program default 0)

TAFIX table of smoothed weighting factors replacing the program generated table in the same order of increasing span stations

The program is constructed so that successive runs may be made with a given program entry. To make additional runs it is only necessary to add an identification record and namelist data that is to be changed from the previous run. An additional capability is provided by the entry NEWDES. When the program is run in the design mode and NEWDES is set to 1, a design camber surface will be found, the input set of camber surface ordinates will be replaced by camber surface ordinates for the new design,and this new design will be treated as an evaluation case. Thus, when the NEWDES option is employed, successive runs may be employed to evaluate the new surface at off-design conditions.

The wing design camber surface ordinates are printed for a reference angle of attack defined by an entry of ALPZPR (reference angle of attack) or CLZPR (reference lift coefficient). The program default is ALPZPR = 0.0. When CLZPR is specified, the program will calculate the corresponding ALPZPR and use this in determination of ordinates.

If the program user desires, span load distribution data may be printed. If the index IPRSLD is set to 1, section aerodynamic characteristics, including the separate contributions of basic pressure loadings, attainable thrust, and vortex forces for each entry in the angle of

attack table will be printed. This data will be printed only for the evaluation mode or when the NEWDES option is employed in the design mode.

The printed program results include:

(1) An iteration-by-iteration history of the convergence parameters for the longitudinal perturbation velocity solution. In the design mode, data is given only for the most critical of up to 44 surfaces which may be employed and for the flat surface at one degree angle of attack. For the supersonic solution in which iteration is not employed, this printout is omitted.

(2) A listing of the spanwise distribution of the leading-edge surface factor, the angle of attack range for full thrust, and the angle of attack for zero thrust. This data is given for the evaluation mode and for all iterations in the design mode from the first (input surface) to the last (optimized surface). For the evaluation mode leading-edge surface factors will all be zero.

(3) A listing of overall wing aerodynamic characteristics as a function of angle of attack. This data is given for the evaluation mode and for all iterations in the design mode from the first (input surface) to the last (optimized surface).

(4) A listing of the spanwise distribution of wing section aerodynamic characteristics including the separate contributions of basic pressure loadings, attainable thrust, and vortex forces. This data will be given only for the evaluation mode (or when the NEWDES option is employed in the design mode) and will be given only if the print option IPRSLD is set to 1.

(5) A listing of the wing surface ordinates as a function of chord position for each of the span stations employed in the program solution.

(6) Listings of pressure distributions for the camber surface at zero angle of attack and for the flat surface at one degree angle of attack.

(7) When the NEWDES option is employed the program will provide a listing of the leading-edge factors used in the design and a listing of suggested replacement values which may lead to improved performance. Generally, the need for this replacement will arise only when it has not been

possible to provide a sufficiently detailed numerical representation of the wing to give closely matched aerodynamic characteristics in the design and evaluation modes.

PROGRAM APPLICATION

Several sample problems have been chosen to point out some of the applications of the present computer program to the design of wing camber surfaces. In some cases, results given by this program will be compared with results of other numerical design methods. The use of the analysis mode of the program will not be covered because the analysis methods differ only in minor detail from methods for which extensive correlations of program data and experimental data have been given; see references 1 and 4 for some examples.

The first two examples of the program application will be used to compare results given by this design method with results given by established methods. For this purpose, only sharp leading-edge wings which generate no leading-edge thrust may be considered. Sharp leading-edge results may be obtained in the present program by setting the leading-edge radius to zero or by using a design Reynolds number of zero.

Figure 6 shows program-generated camber surface data for a wing planform typical of a subsonic transport. The design conditions are a Mach number of 0.8, and a lift coefficient of 0.35 with no restraint on the pitching moment. Camber surface ordinates nondimensionalized with respect to the wing root chord are shown as a function of distance from the leading edge also nondimensionalized with respect to the root chord. These data, which are shown for five semispan stations from 0.1 to 0.9, are compared with results for the same conditions given by the method of reference 8 and with ordinates for a flat wing developing the same lift coefficient. It is seen that the camber surfaces given by the two design methods are similar in character; the main difference occurring in the root chord region aft of the leading edge. Because of fundamental differences in the two design approaches, identical results could not be expected. The similarity of results is believed to be indicative of a proper functioning of the present design method.

Program lifting pressure distribution data for the subsonic transport wing design are shown in figure 7. Generally, the lifting pressures are distributed rather uniformly over the planform. One of the goals of the design process is the elimination of leading-edge pressure singularities that

are not associated with the generation of attainable thrust. For this sharp-leading-edge wing design, singularity strengths should be reduced to zero. The pressure distributions, however, show residual singularity strengths corresponding to those generated by a flat wing of the same planform at one half of one degree angle of attack or less. This discrepancy, though relatively minor, shows the sensitivity of the pressure loadings to details of the camber surface shape. For normal flight conditions, even a very small leading-edge radius would insure that these residual singularities would be translated into fully attainable leading-edge thrust. The leading-edge radius thus would provide a margin of safety for the design.

Program-generated force data for this first example are shown in figure 8. Drag coefficients given in the program design mode (obtained by superposition of 20 individual candidate surfaces) were found to agree closely with drag coefficients given in the program evaluation mode (obtained by activating the NEWDES feature which consolidates all the candidate surfaces into one surface). The program results are compared with theoretical limits for a flat wing with no thrust $(C_L \tan(C_L/C_{L,\alpha}))$ and for a twisted and cambered wing with an elliptical span load distribution $(C_L^2/\pi AR)$. As shown in the figure, this program gives a slightly higher drag at the design conditions than does the method of reference 8. In part, this occurs because the present method uses a sine rather than a tangent variation of lifting pressure with incidence angle. Both programs show a design point value close to the theoretical lower bound.

Consideration of supersonic camber surface design applications disclosed the problem of a lack of correspondence of drag values given in the program design and evaluation modes. The problem is traceable to numerical instabilities caused by the rectangular element wing representation which are discussed in the section entitled "Analysis Methods." A means of circumventing this problem will be discussed with the help of the second example which treats a 70° swept leading-edge arrow wing in supersonic flow.

Figure 9 (a) shows program generated force data for the arrow wing camber surface design at a Mach number of 2.05 and a lift coefficient of 0.16 with no restraint on the moment. The program data is compared with the same upper and lower bounds as used for the subsonic flow case. At supersonic speeds, however, the lower bound can not be approached as closely because of the

presence of wave drag due to lift. The evaluated drag values are seen to be appreciably higher than the design values. This can occur because the data provided in the design mode is based on the addition of surface ordinates and aerodynamic coefficients for, in this case, 35 different candidate surfaces, each of which may introduce numerical calculation errors. The optimization process will take advantage of any errors which favor lower drag without regard to the validity of the results, and thus the drag values given in the design mode may be unrealistically low. Subsequent evaluation of that surface by use of the program NEWDES feature will give more realistic results. But, of course, the surface subject to that evaluation may differ appreciably from a true optimum surface. As shown in sketch (q), an increase in the number of wing elements which is controlled by the program entry JBYMAX will, in general, reduce the discrepancy. In the sketch, the suction parameter S_S is shown as a function of the reciprocal of the JBYMAX term. As JBYMAX and the number of wing elements become very large (small values of the reciprocal), it is seen that design and evaluation suction parameters approach each other. However, even for the largest permissible program value of JBYMAX (30) there are appreciable differences. A less severe limitation on JBYMAX as in the original supersonic programs of reference 5 would help, but would not completely solve the problem.

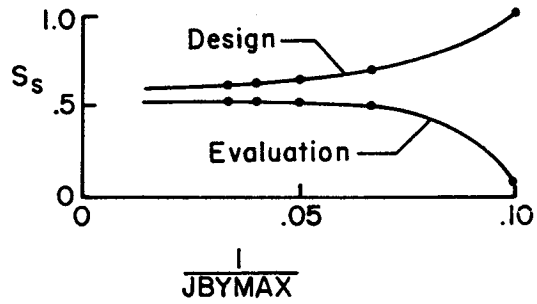

Sketch (q)

A means of arriving at a valid design, in spite of the discrepancies just discussed, was given in the description of the design method. In order to clarify the strategy employed, the application of the procedure to this particular problem will be illustrated.

Recall that one of the objectives of the design procedure is to provide the proper relationship between the leading edge surface slope and the local upwash and that this is accomplished by creating a surface whose angle of attack for zero thrust distribution matches the design goal, in this case the design angle of attack. The angle of attack for zero thrust distribution as used in the design and a more accurate distribution by the evaluation for this

example are shown in sketch (r). Looking first at the design distribution, it is seen that numerical instabilities at inboard span stations where relatively few elements influence the solution prevent a close match with the design goal, but that the match becomes better with increasing span station as more and more elements enter into the solution. This trend continues until the wing chord becomes too small to accommodate the number of elements required for effective application of program smoothing techniques. Notice that the evaluation distribution gives appreciably higher values of α_{zt}. This discrepancy decreases with an increasing number of span stations, indicating that if a sufficiently large number of elements could be employed so as to reduce apex and tip region discrepancies to insignificance, the design goal could effectively be met. That resolution of the problem, however, is not practical. The remedy applied here is to change the design goal by the difference between that goal and the evaluated α_{zt} distribution.

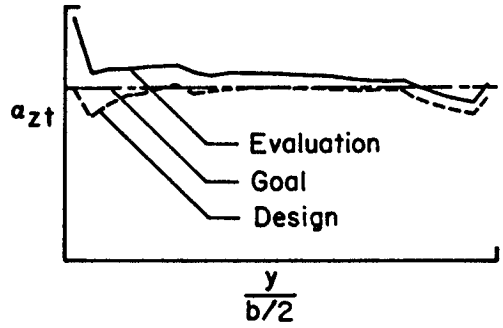

Sketch (r)

As shown in sketch (s), there is also a failure in the matching of the evaluated optimum lift coefficient to the design lift coefficient. Since the primary control over the design lift coefficient is in the leading-edge shape, a correction can be effected by modifying the magnitude of the distribution of leading-edge surface factors.

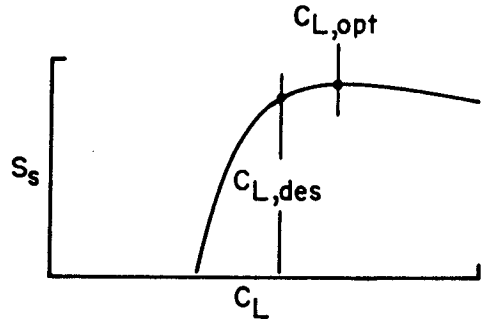

Sketch (s)

The following correction has been found to be effective in compensating for both of the preceding deficiencies:

$$A_{le,\ adj} = \frac{C_{L,des}}{C_{L,opt}} \left[\frac{A_{le} \times 1^{\circ} + \alpha_{zt,\ goal} - \alpha_{zt,\ eval}}{1^{\circ}} \right]$$

Sketch (t) shows the leading edge surface factor used in the design, the suggested adjusted factors which may be expected to result in improved performance, and a fairing of the adjusted factors to assure a smooth camber surface. The program provides a listing of the suggested adjusted factors, but the program user will have to supply the fairing. A rerun of the program with tabulated input of the new leading edge surface factors (TAFIX) will generally give a camber surface with improved performance and a surface relatively free of irregularities. Although the program can be used satisfactorily in a hands-off fashion, the occasional need for reruns and the general iterative nature of the solution make the method a logical candidate for interactive graphic implementation.

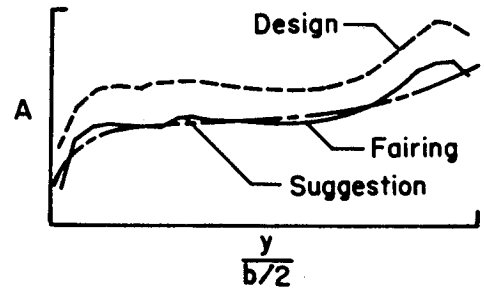

Sketch (t)

Force data for a new design with adjusted leading edge surface factors is shown in figure 9(b). The evaluated aerodynamic characteristics of the revised design show a modest improvement over the original design (a reduction of 0.0004 in C_D or an increase of 0.04 in S_s at the design C_L) for a camber surface now without irregularities. A difference between design and evaluation aerodynamic characteristics will indicate the need to consider the use of the adjustment technique, and although in this case the change was relatively small, it will not always be so. Figure 10 shows the camber surface for the revised design and allows it to be compared with a surface described in reference 9 which was determined by an optimum combination of three candidate pressure loadings. The two camber surfaces are seen to be similar, particularly the critical camber surface slopes near the leading edge. Lifting pressure distributions for this design are shown in figure 11. These distributions are generally rather uniform and are smooth except in the immediate vicinity of the leading edge. Leading-edge pressures show residual singularities as did the distributions of the previous subsonic example, and also display additional irregularities. Reasons for irregularities in the supersonic solution are discussed in the section of the paper dealing with basic loadings at supersonic speeds. The present method, which is based on an optimum combination of surfaces, generates smooth camber

surfaces but displays irregularities in leading-edge pressures. In contrast, the method of reference 5, which is based on an optimum combination of loadings, gives smooth pressure distributions but displays irregularities in the leading-edge camber surface. In either case, a reasonable solution is obtained in spite of the irregularities.

Attention will now be given to wings with thickness and leading edge radii, which offer leading edge thrust benefits that the present design method attempts to utilize. A supersonic fighter wing planform will be used to demonstrate the use of the design method in attempting to define the mildest possible camber surface which will yield aerodynamic performance comparable to that attainable with full theoretical leading-edge thrust. This approach appears to be particularly appropriate for supersonic speeds because of the nonlinear increase of drag penalties with camber surface severity (see reference 10).

Aerodynamic data for a supersonic fighter wing with a rounded leading edge for the inboard wing panel are shown in figure 12(a). The design conditions are $M = 2.0$, $R = 37 \times 10^6$, $C_{L,des} = 0.24$, and $C_{m,des} = 0.0$. As for the previous arrow wing design, there are discrepancies between the program design mode and the program evaluation mode. Thus, consideration of the leading edge surface factor adjustment previously discussed for the arrow wing example is also appropriate here.

Sketches (u) to (w), which are similar to sketches (r) to (t) used in the description of the process as applied to the arrow wing example, may be used to point out differences due to the change in the design goals. As shown in sketch (u), the α_{zt} goal is equal to the design angle of attack only for the outer portion of the wing semispan where the supersonic wing leading edge prevents the development

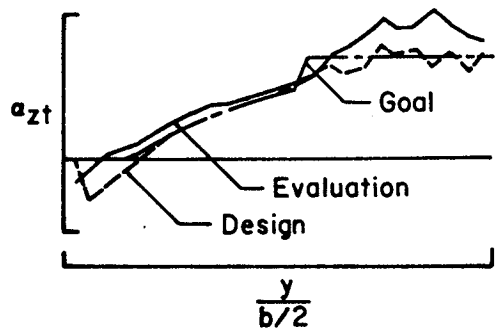

Sketch (u)

of any leading-edge thrust. For the inboard portion of the wing, the goal α_{zt} is equal to $\alpha_{des} - \Delta\alpha_{ft}$ or 0.0 whichever is greater. As in the previous example, α_{zt} as evaluated fails to meet the goal and as shown in sketch (v), $C_{L,opt}$ differs from $C_{L,des}$. The suggested leading-edge surface factors and the fairing employed are shown in sketch (w).

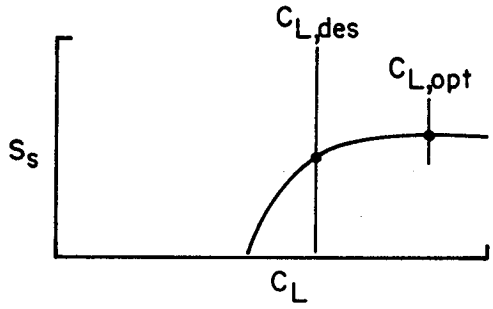

Sketch (v)

Aerodynamic data for the supersonic fighter wing design with the leading-edge surface factor adjustment are shown in figure 12(b). The change in the evaluated drag coefficient at the design lift is about 0.0016 or about 0.08 in S_s. The design camber surface is shown in figure 13. There is seen to be a significant amount of twist but relatively little camber except for wing semispan stations just inboard of the leading-edge break (y/(b/2) = 0.57) where the wing leading edge is subsonic and where there is a strong upwash field but little potential for the development of leading-edge thrust.

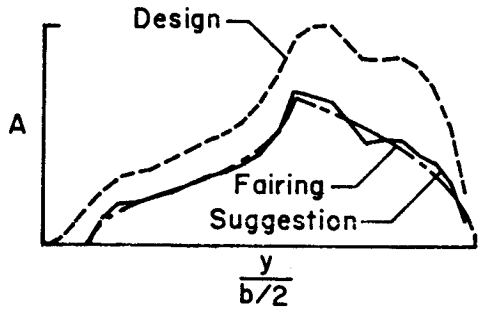

Sketch (w)

An extension to this example may be used to show how the program may be used for special purpose design, in this case a mission adaptive wing surface, by appropriate selection of candidate surfaces. In this problem, the previous camber surface designed for supersonic cruise will be subjected to a redesign at a subsonic Mach number of 0.8. The redesign, however, will be constrained so that only selected areas of the wing in the vicinity of the leading and trailing edges will be altered. These redesign areas are shown in the sketch in the upper part of figure 14(a). The limitation of the design area is accomplished by setting the number of general candidate camber surfaces to zero and by the input of appropriate tables of leading-edge and trailing-edge chord. Aerodynamic results generated in the design process are shown in the lower part of figure 14(a). It should be noted first that the supersonic camber surface evaluated at the subsonic design condition has significantly

better aerodynamic performance than a flat wing of the same planform. Modification of the leading and trailing edge regions alone is seen to produce additional performance gains. Fairly severe restrictions on the design, however, prevent a close approach to lower bound drag levels. Figure 14(b) affords a comparison of the original and the redesigned camber surface. It will be noted that leading edge region changes are quite pronounced, but that trailing edge surface changes are mild.

An example of a supersonic transport wing design has been chosen to illustrate the effect of leading-edge radius on camber surface design. Program data are shown in figure 15(a) for a wing with a thickness ratio of 3 percent, at a design Mach number of 2.7 for three designs. For the first design, the leading edge is considered to be sharp and the design lift coefficient is set equal to the anticipated cruise C_L of 0.10. Because such a design is known to introduce nonlinear drag penalties as a function of design C_L, it has become common practice (see for example reference 10) to reduce the design lift coefficient. The design lift coefficient of 0.05 produces a milder camber surface and although a higher theoretical drag is indicated than for the 0.10 design, the lowered design C_L can be expected to give an actual improvement. A third design alternative is offered by the method of this report. For this design, the full cruise lift coefficient of 0.10 is used as the design value and a moderately rounded leading edge ($r/c = 0.00034$ for the inboard 75 percent of the semispan) with its ability to produce thrust is used to define a mild camber surface. In general, this surface is no more severe than the surface for the $C_{L,des} = 0.05$ sharp leading edge design shown in figure 15(b). It has an appreciable amount of twist but has only mild curvature of section camber lines. The theoretical drag is essentially identical to that of the sharp leading edge $C_{L,des} = 0.10$ design. Thus there is a possibility that such a design could out-perform the rule-of-thumb design with $C_{L,des}$ equal to about half the cruise C_L.

For all of the previous application examples, it has been assumed that the primary purpose of the design has been to produce drag levels comparable to those attainable with full theoretical leading-edge thrust with as mild as possible a camber surface. This approach is obviously applicable to supersonic design because of the nonlinear nature of the camber drag. There is another design approach that may be considered when good performance must

be maintained over a wide range of lift coefficients. In that case an intermediate lift coefficient may be selected as the design value and the benefits of attainable thrust can extend good performance over a wider range of lift coefficients. Such an example for a general aviation wing design is shown in figures 16 and 17. A sharp leading edge design was obtained for a Mach number of 0.5 and a design lift coefficient of 0.35. This surface was then evaluated for a Reynolds number of 2.8×10^6 to find the C_L range for full theoretical thrust. As may be noted, this range extends from about $C_L = -0.3$ to $C_L = 0.9$. If desired, this range could be shifted up or down by redesigning for a new lift coefficient.

The present wing design method is based in part on notes for the design of low speed flap systems presented in reference 2. This design method now provides an improved means of selecting flap systems.

The final example will illustrate how the present wing design computer program can be combined with the computer program of reference 2 for the design and analysis of wing flap systems. The problem is to devise an efficient set of leading-edge flaps and trailing-edge flaps for the wing shown in the sketch at the top of figure 18 for flight conditions of $M = 0.8$, $R = 50.0 \times 10^6$, and $C_L = 0.5$. Only the regions of the wing within the dashed lines are available for flaps. The remainder of the wing is assumed to be a flat surface. The first step is the design of an overall wing camber surface for the flight conditions. This surface is shown as a solid line in the ordinate plots of figure 18. For convenience,the camber ordinates are shown for the zero angle-of-attack condition rather than the design lift coefficient condition. The problem is to define a flap system which will approximate the camber surface and will approach the cambered wing performance. It is assumed that the leading-edge flaps can be segmented but the trailing-edge flaps cannot. The surface of the wing with a candidate set of flaps is shown as the dashed line. For this example, the leading-edge flap chords cover the full available chord for the outer half of the flap but are smaller for the inboard portion. For thicker wings or higher Reynolds numbers, the camber surface curvature would be reduced and further reduction of inboard chords could be made.

The candidate flap system planforms and deflection schedules are shown in the sketches of figure 19. This figure also shows wing suction parameters

evaluated by the program of reference 2 for various combinations of leading-edge and trailing-edge flap deflection factors. From this plot, the candidate flap system appears to offer the best aerodynamic performance for a leading-edge flap deflection factor of about 1.1 and a trailing-edge flap deflection factor of about 0.6. The optimum leading-edge flap deflection factor near a value of 1.0 indicates that the fitting of the camber design surface shown in figure 18 provided a reasonable estimate of the flap deflections necessary for optimum performance. Program estimates of the wing-flap system aerodynamic characteristics for these deflection factors are shown in figure 20. The design point suction parameter of 0.86 for the flap system compares with a suction parameter for 0.97 for the smooth camber surface. Notice the effect of attainable thrust in producing drag levels that parallel the $C_L^2/\pi AR$ lower bound for an appreciable range of lift coefficients. Also note the sharp break away from the lower bound curve immediately above the design lift coefficient, which is characteristic of the attainable thrust design method. Program lifting pressure distributions for the flap system and for the camber surface on which the flap design is based are shown in figure 21. The most noticeable difference occurs in the region of the flap hinge lines where the flap loadings display singularities. These pressure peaks indicate that the flap system would be more sensitive to low Reynolds number flow separation than would the camber surface.

If leading-edge flap segmentation is not permitted, the flap design problem becomes more difficult. For a straight hinge line and constant leading-edge flap deflection, it may not be possible to define flap surfaces that reasonably approximate the wing design camber surface. One way of handling this problem is to use the program of reference 4 to evaluate a limited series of candidate flaps and from this data select an optimum for that series. For the wing of the example just treated, it is clear from the design data that the flap chord of the wing tip should be as large as the design limitations allow. The remaining problem is the selection of the hinge-line sweep angle. Flap program results indicate that the hinge-line should be at the rear limit of the available flap area and that optimum flap deflection angeles are about 15 degrees for the leading-edge flaps and about 6 degrees for the trailing-edge flaps. These deflections produce a suction parameter of about 0.82 at the $C_L = 0.5$ design condition. As might have been expected, this aerodynamic efficiency is somewhat less than that indicated for

the segmented leading-edge flaps.

Although the present wing design program and the wing and flap evaluation program of reference 2 account for the effects of Reynolds number on leading-edge thrust achievement there are other detrimental effects of low Reynolds numbers that are not taken into account. Thus the performance estimates given in this report are actually potential levels that may be approached if the Reynolds number is high enough. A more complete discussion of the effects of Reynolds number on wing performance is given in reference 2.

All of the program application examples shown here have been for isolated wings, and thus have avoided complex problems associated with complete configuration design. Studies of means of integrating fuselage-wing configurations so as to preserve as much as possible of the wing design benefits have been treated in references 11 and 12. Generally, the principle involved is the arrangement of the fuselage so as to disturb as little as possible the optimized distribution of lifting forces given by the wing design method. References 11 and 12 give some guidance for the integration of other airplane components. These studies were concerned with the supersonic speed region where interference effects can become critical. The general principles, however, should be applicable at subsonic speeds.

CONCLUDING REMARKS

This paper has described methodology and an associated computer program for the design of wing lifting surfaces with attainable thrust taken into consideration. The approach is based on the determination of an optimum combination of a series of candidate surfaces rather than the more commonly used candidate loadings. Special leading-edge surfaces are selected to provide distributed leading-edge thrust forces which compensate for any failure to achieve the full theoretical leading-edge thrust, and a second series of general candidate surfaces are selected to minimize drag subject to constraints on the lift coefficient and, if desired, on the pitching moment coefficient. A primary purpose of this design approach is the introduction of attainable leading-edge thrust considerations so that relatively mild camber surfaces may be employed in the development of aerodynamic efficiencies comparable to those attainable if full theoretical leading-edge thrust could

be achieved. The program provides an analysis as well as a design capability and is applicable to both subsonic and supersonic flow.

A series of examples have been given to illustrate the applicability and limitations of the design method, and to compare program results with those of established design methods. For the design of sharp leading edge wings which can be handled by previously existing methods, there was seen to be a general agreement between the solutions given by the present and previous methods. Some examples were given to illustrate the new capability for the design of high performance wings with relatively mild camber surfaces resulting from utilization of attainable leading edge thrust. Examples illustrating the special capability of the program for the design of mission adaptive surfaces and selection of flap systems were also given. It was noted that in some cases, particularly at supersonic speeds, the program may require more than one run to produce a solution that is sufficiently close to a true optimum. However, a means of correcting this deficiency by a simple adjustment so that only one additional computer run is required was demonstrated. Although the program can be used satisfactorily in a hands-off fashion, this problem and the general iterative nature of the solution make the method a logical candidate for interactive graphics implementation.

References

1. Carlson, Harry W.; Mack, Robert J.; and Barger, Raymond L.: Estimation of Attainable Leading-Edge Thrust for Wings at Subsonic and Supersonic Speeds. NASA TP-1500, 1979.
2. Carlson, Harry W.; and Walkley, Kenneth B.: An Aerodynamic Analysis Computer Program and Design Notes for Low Speed Wing Flap Systems. NASA CR-3675, 1983.
3. Stevens, J. R.: A New Lifting Surface Approach to the Design of Supersonic Wings. Design Conference Proceedings—Technology for Supersonic Cruise Military Aircraft, Volume 1, AFFDL/FX, U. S. Air Force, 1976.
4. Carlson, Harry W.; and Walkley, Kenneth B.: A Computer Program for Wing Subsonic Aerodynamic Performance Estimates Including Attainable Thrust and Vortex Lift Effects. NASA CR-3515, 1982.
5. Carlson, Harry W.; and Miller, David S.: Numerical Methods for the Design and Analysis of Wings at Supersonic Speeds. NASA TN D-7713, 1974.
6. Carlson, Harry W.; and Mack, Robert J.: Estimation of Leading-Edge Thrust for Supersonic Wings of Arbitrary Planform. NASA TP-1270, 1978.
7. Lan, C. Edward; and Chang, Jen-Fu: Calculation of Vortex Lift Effect for Cambered Wings by the Suction Analogy. NASA CR-3449, 1981.
8. Kuhlman, John M.; and Shu, Jin-Yea: Computer Program Documentation for a Subcritical Wing Design Code Using Higher Order Far-Field Drag Minimization. NASA CR-3457, 1981.
9. Carlson, Harry W.: Aerodynamic Characteristics at Mach Number 2.05 of a Series of Highly Swept Arrow Wings Employing Various Degrees of Twist and Camber. NASA TM X-332, 1960.
10. Carlson, Harry W.; and Mack, Robert J.: Estimation of Wing Nonlinear Aerodynamic Characteristics at Supersonic Speeds. NASA TP-1718, 1980.
11. Carlson, Harry W.; and McLean, F. Edward: Current Methods for Prediction and Minimization of Lift-Induced Drag at Supersonic Speeds. NASA TM X-1275, 1966.
12. Robins, A. W.; Morris, O. A.; and Harris, R. V., Jr.,: Recent Research Results in the Aerodynamics of Supersonic Vehicles. Journal of Aircraft, vol. 3, no. 6, Nov.-Dec. 1966, pp. 573-577.

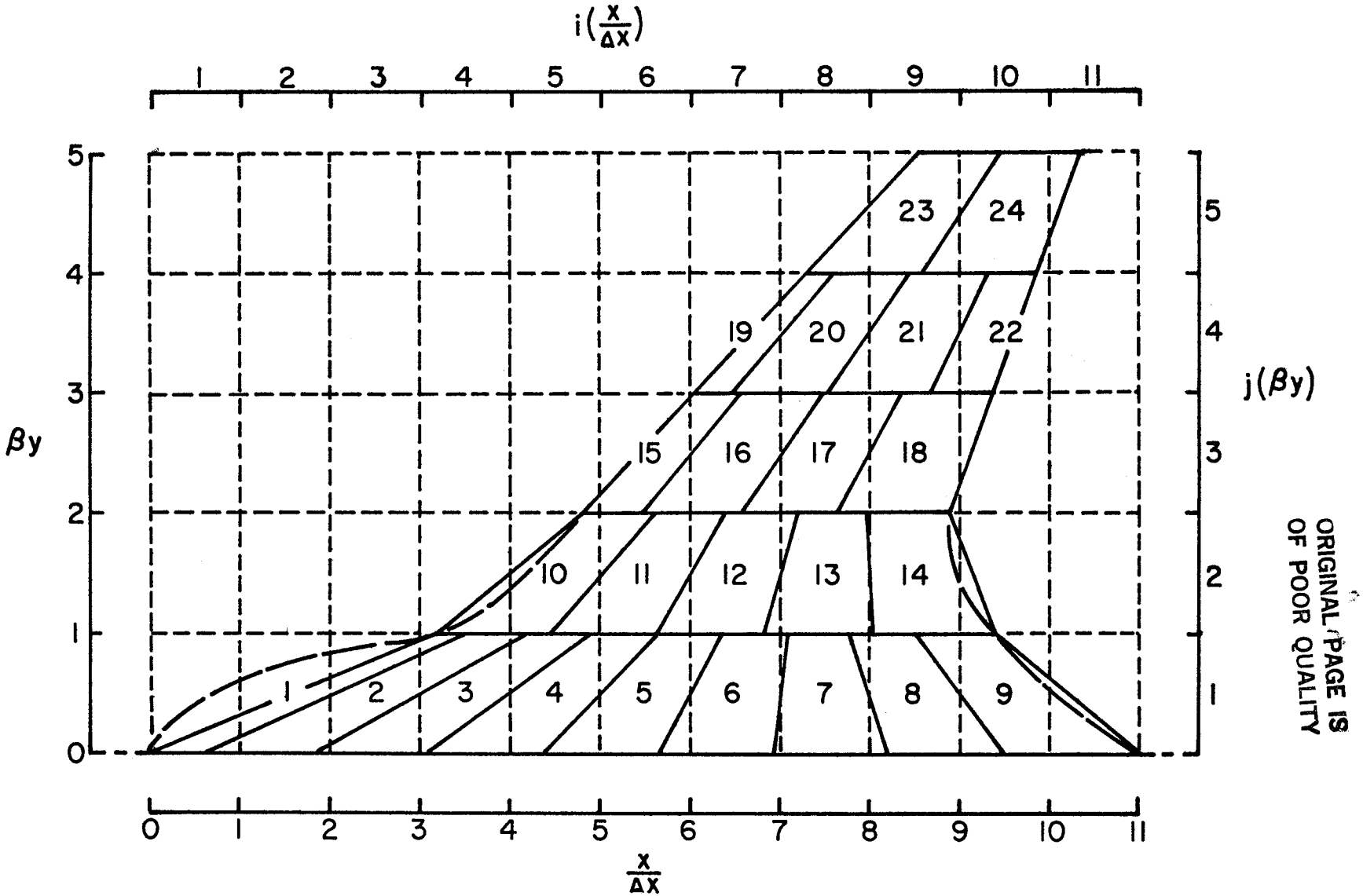

Figure 1.- Grid system used in subsonic analysis.

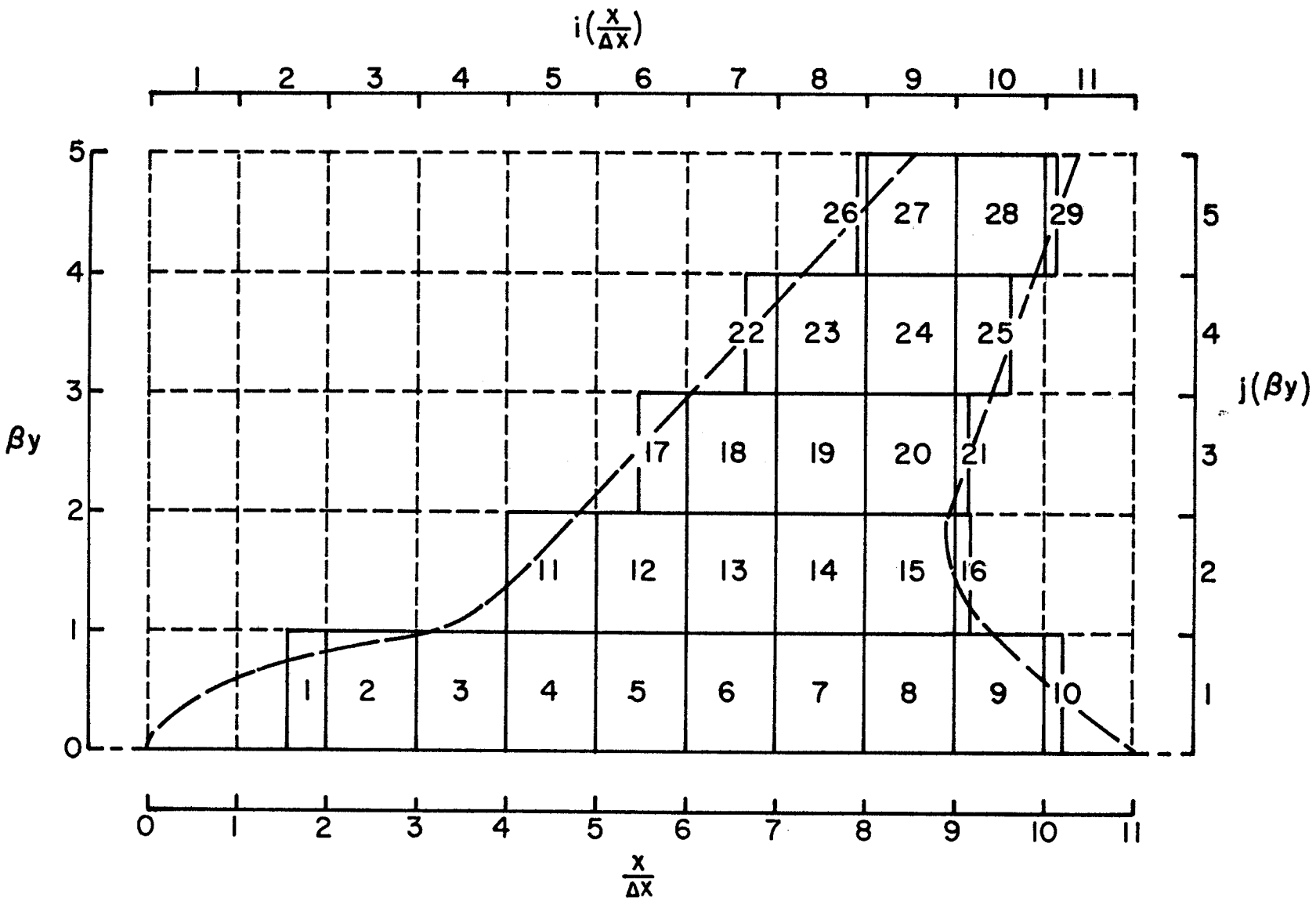

Figure 2.- Grid system used in supersonic analysis.

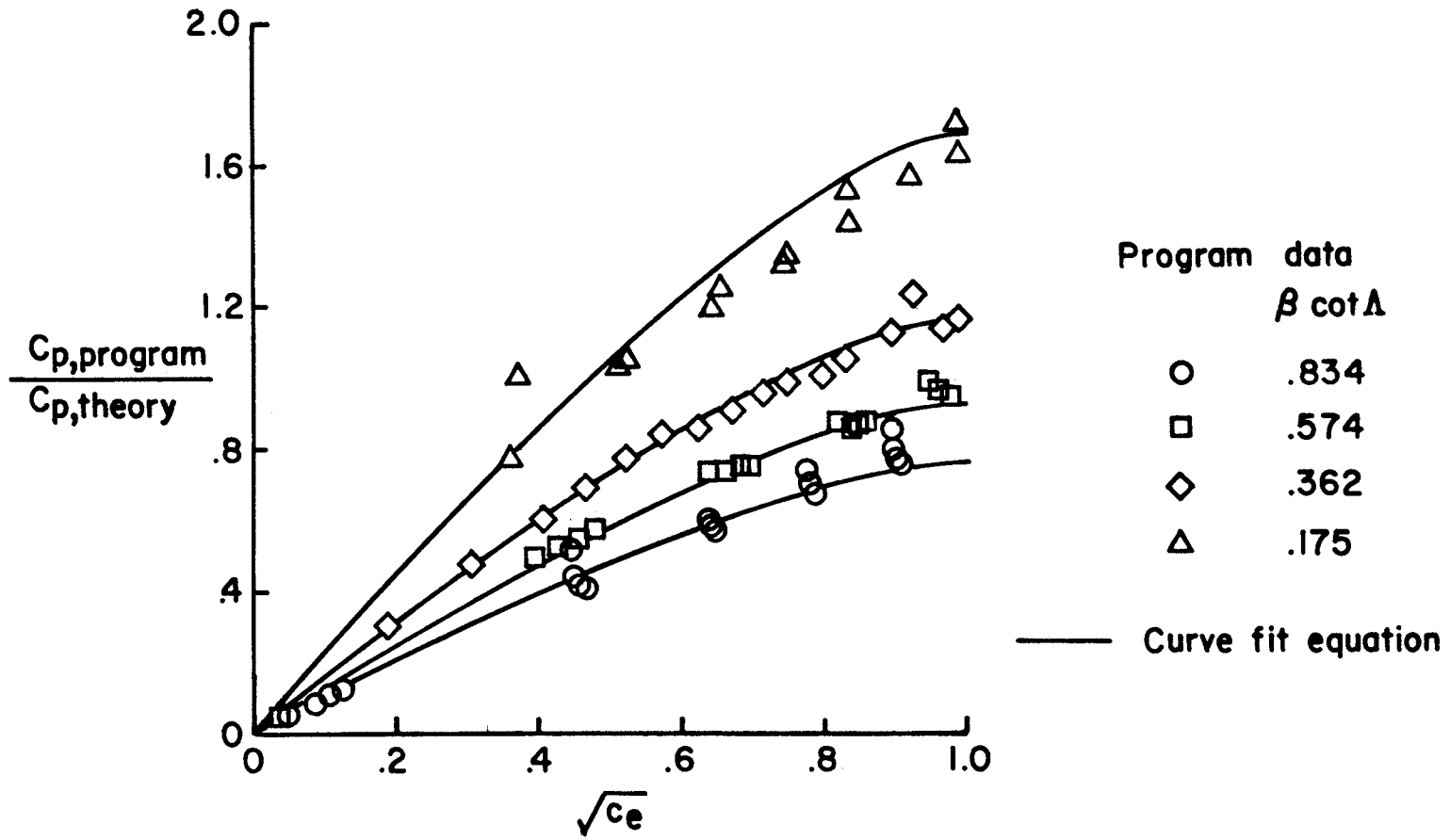

(a) Pressure ratio.

Figure 3.- Supersonic analysis program results for leading-edge elements.

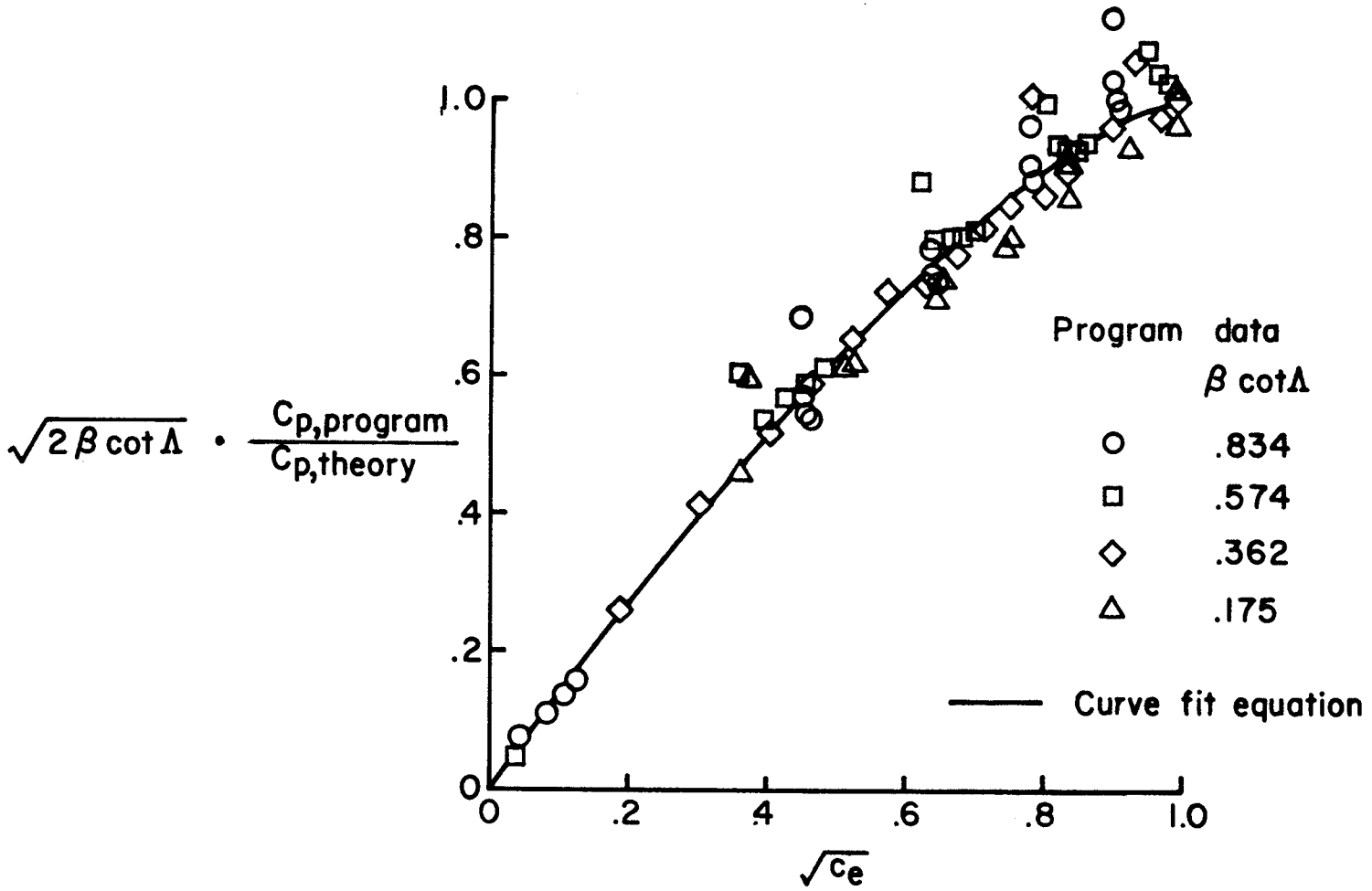

(b) Pressure ratio parameter.

Figure 3. Concluded.

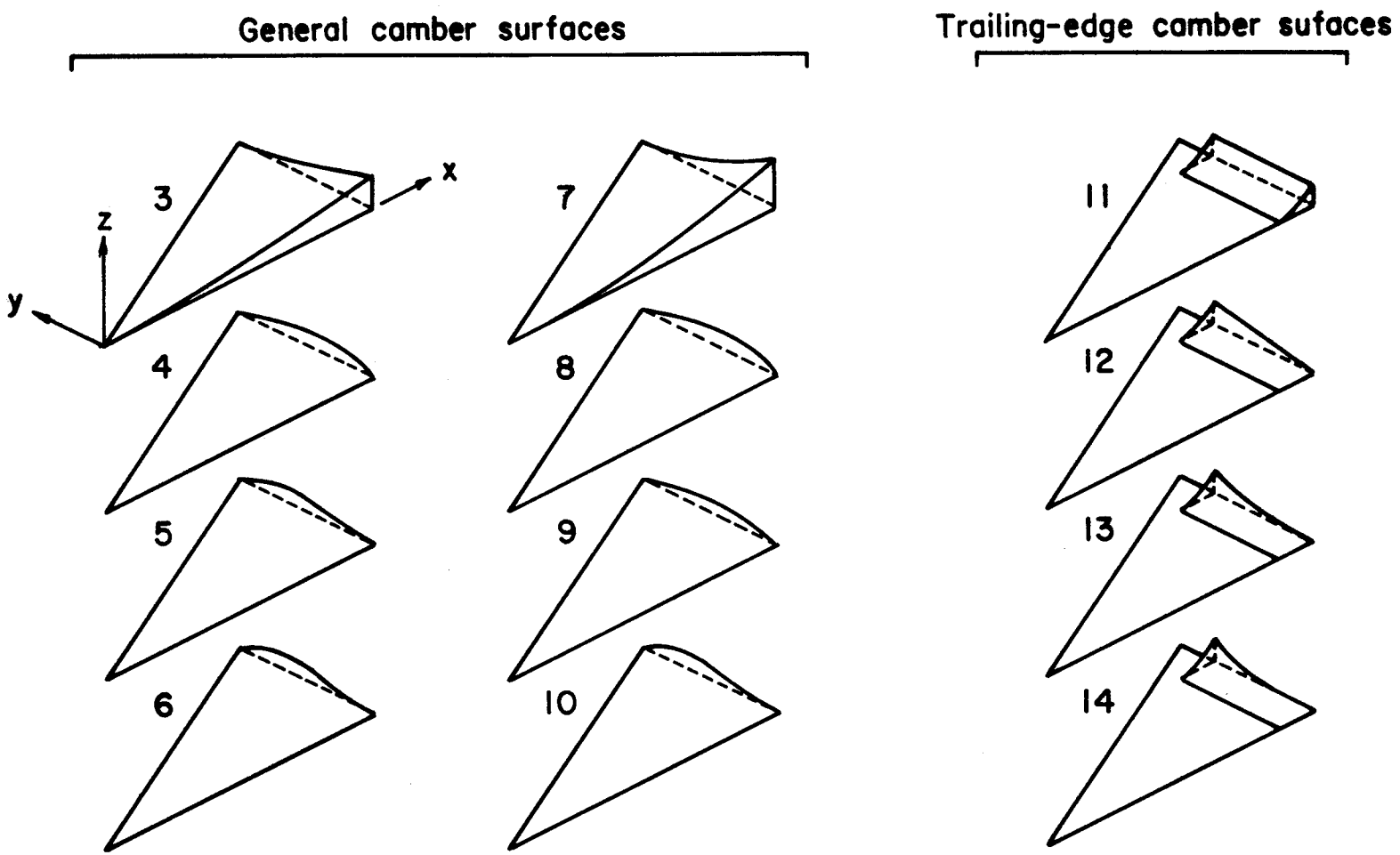

Figure 4.- Typical candidate camber surfaces. Delta wing example, right-hand panel shown.

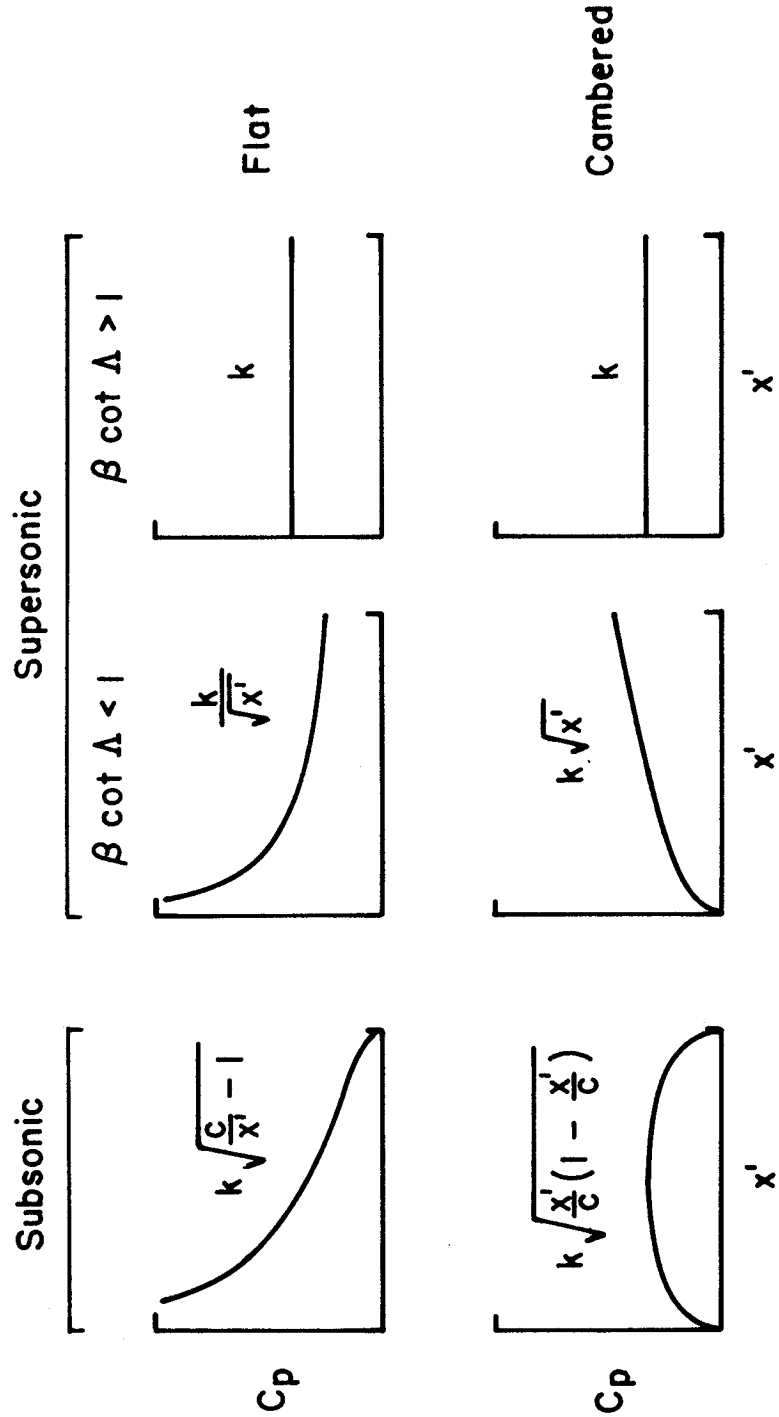

Figure 5.- Pressure distribution forms used for integration.

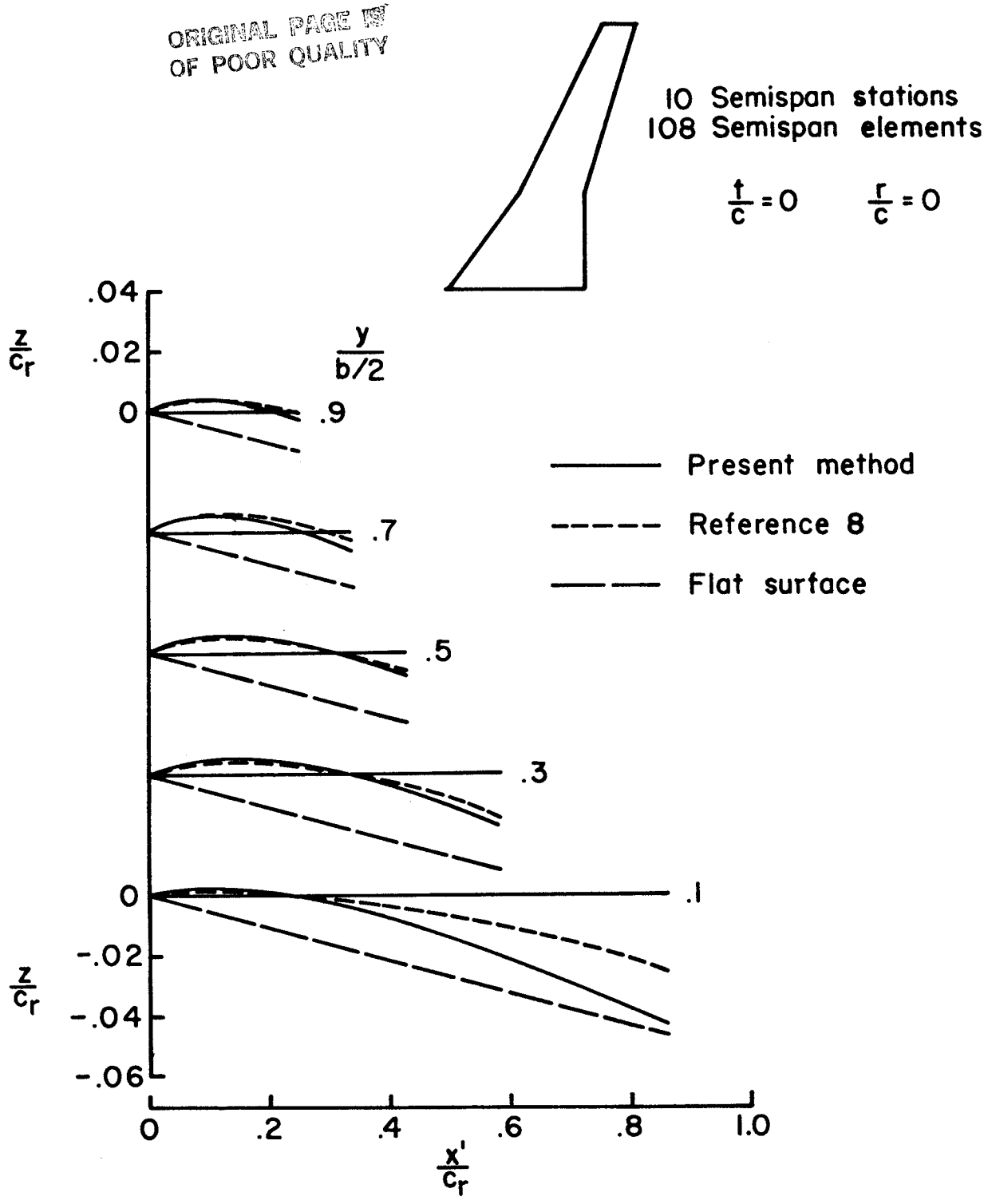

Figure 6.- Program geometric data for a subsonic transport camber surface design. M = 0.8, R = 0.0, $C_{L,des}$ = 0.35, no C_m restraint.

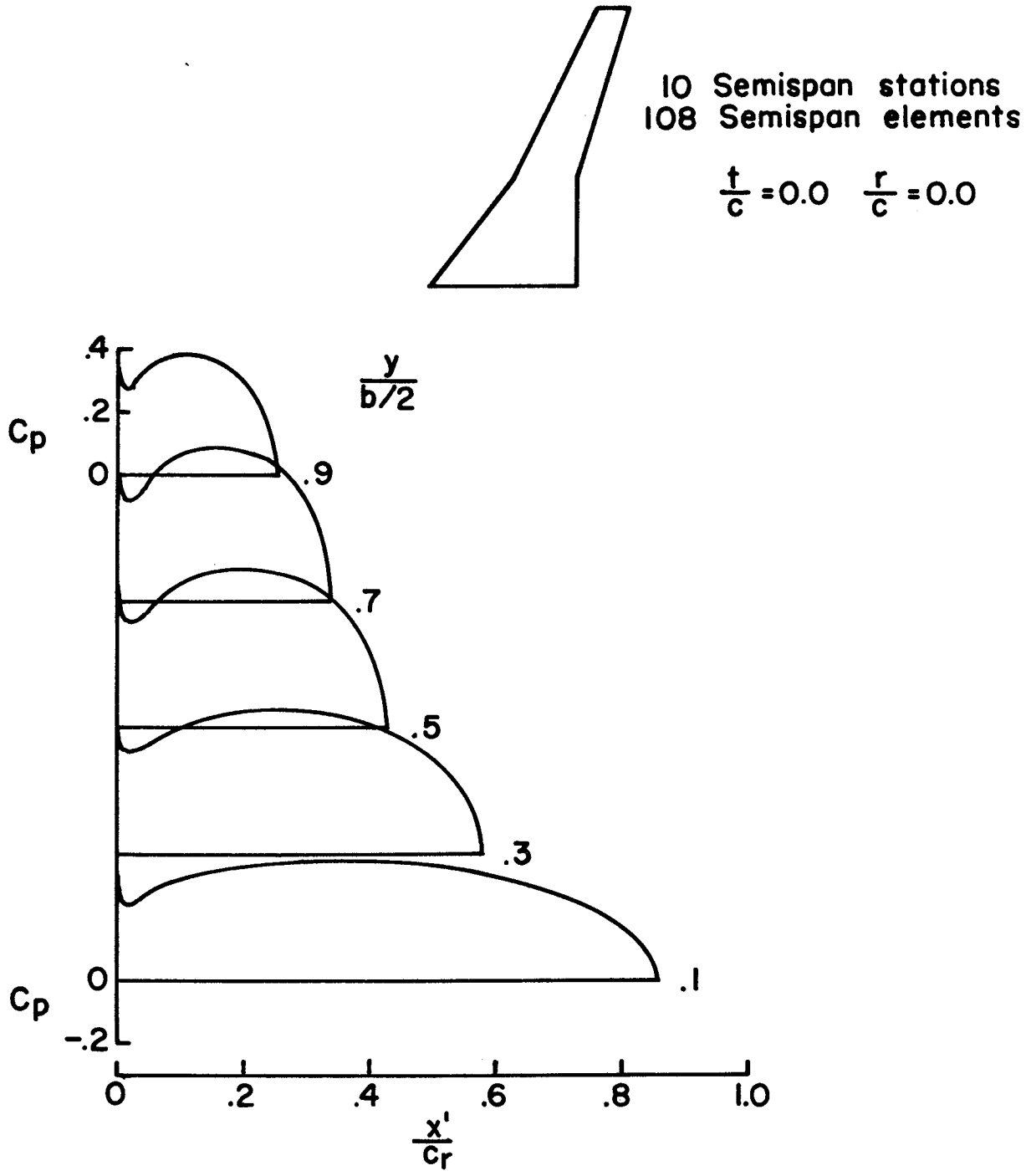

Figure 7.- Program pressure distribution data for a subsonic transport camber surface design. M = 0.8, R = 0.0, $C_{L,des}$ = 0.35, no C_m restraint.

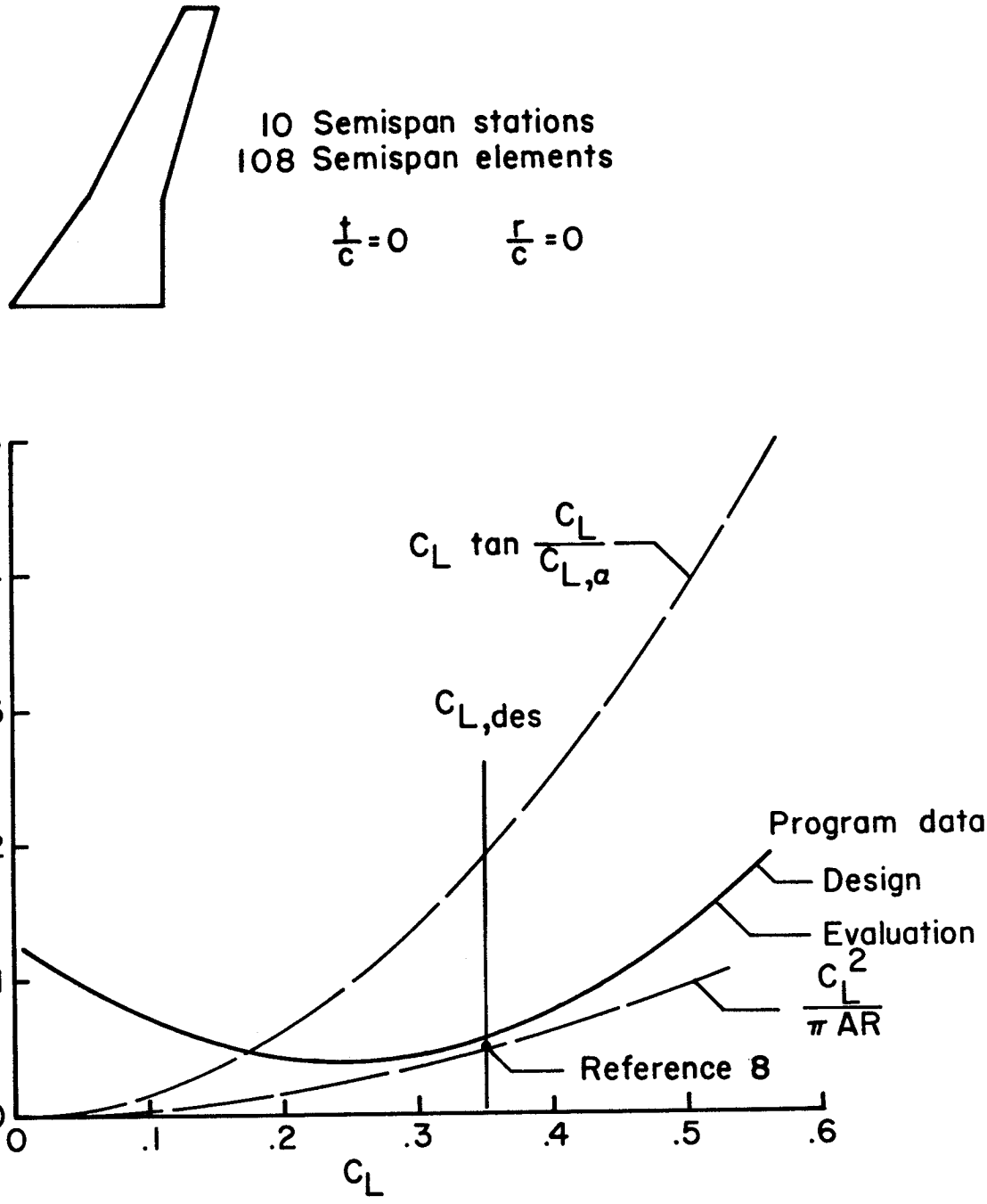

Figure 8.- Program aerodynamic data for a subsonic transport camber surface design. M = 0.8, R = 0.0, $C_{L,des}$ = 0.35, no C_m restraint.

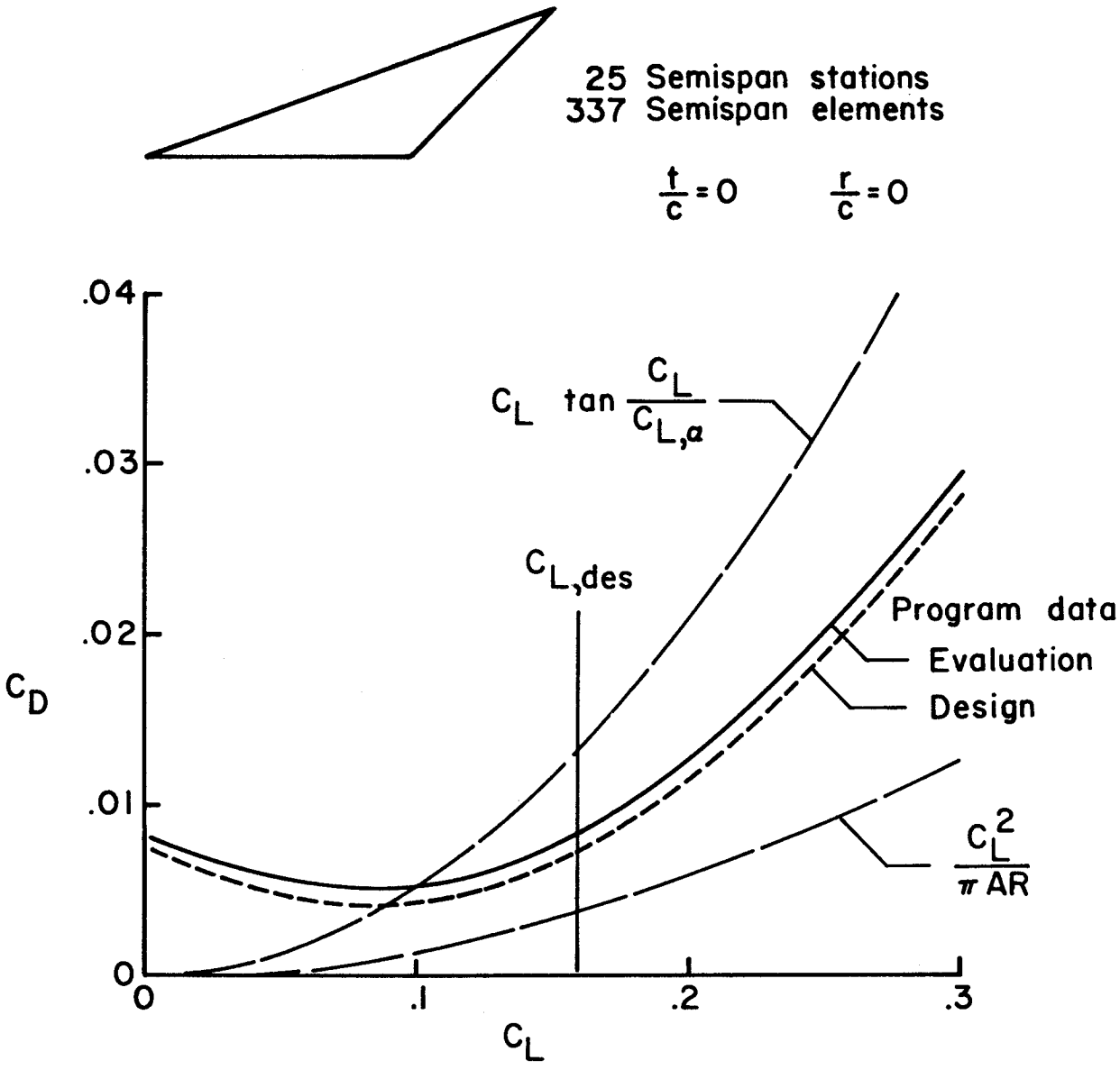

(a) Without adjustment of leading-edge surface factors.

Figure 9.- Program aerodynamic data for a 70° arrow wing camber surface design. M = 2.05, R = 0.0, $C_{L,des}$ = 0.16, no C_m restraint.

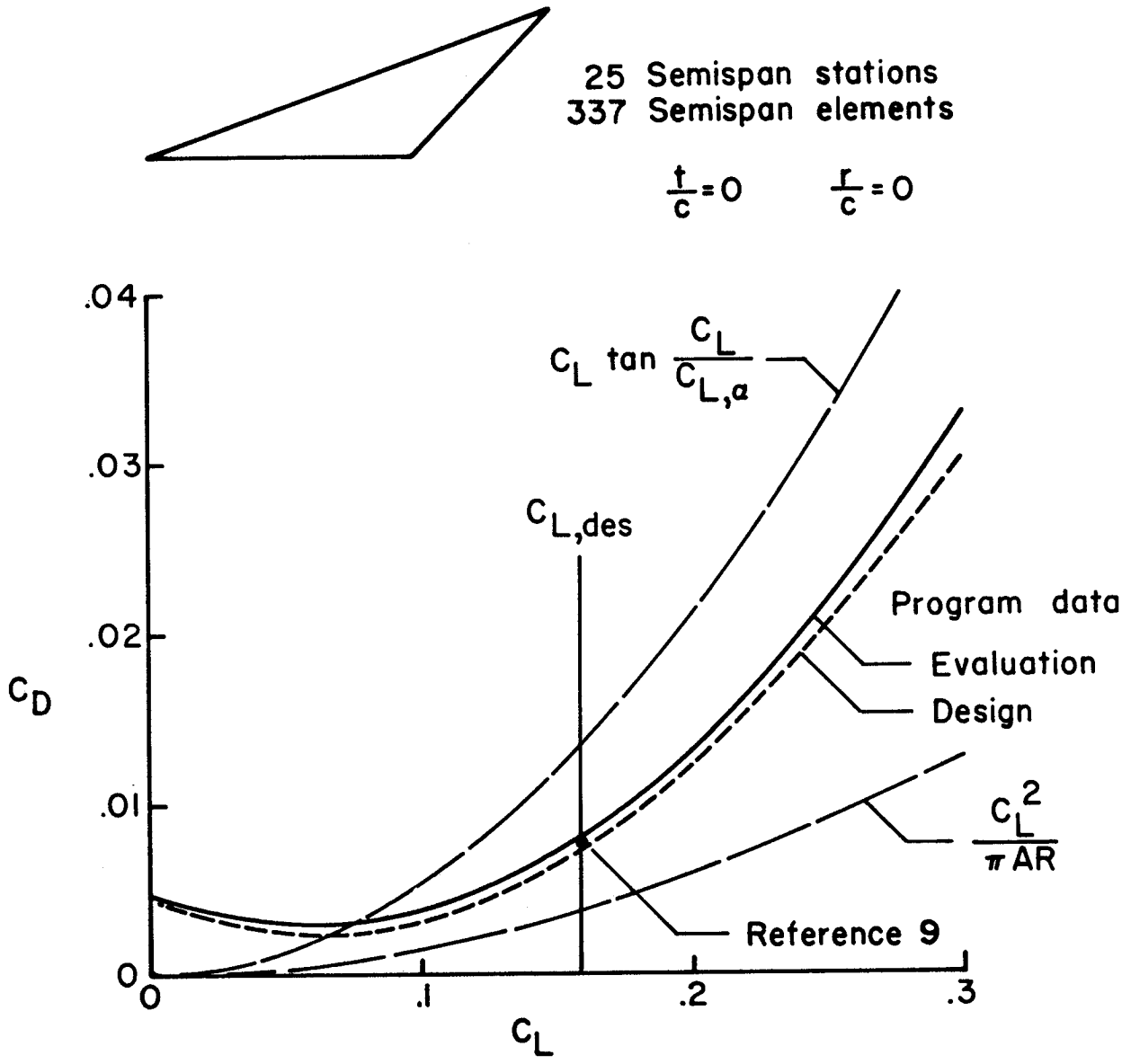

(b) With adjustment of leading-edge surface factors.

Figure 9.- Concluded.

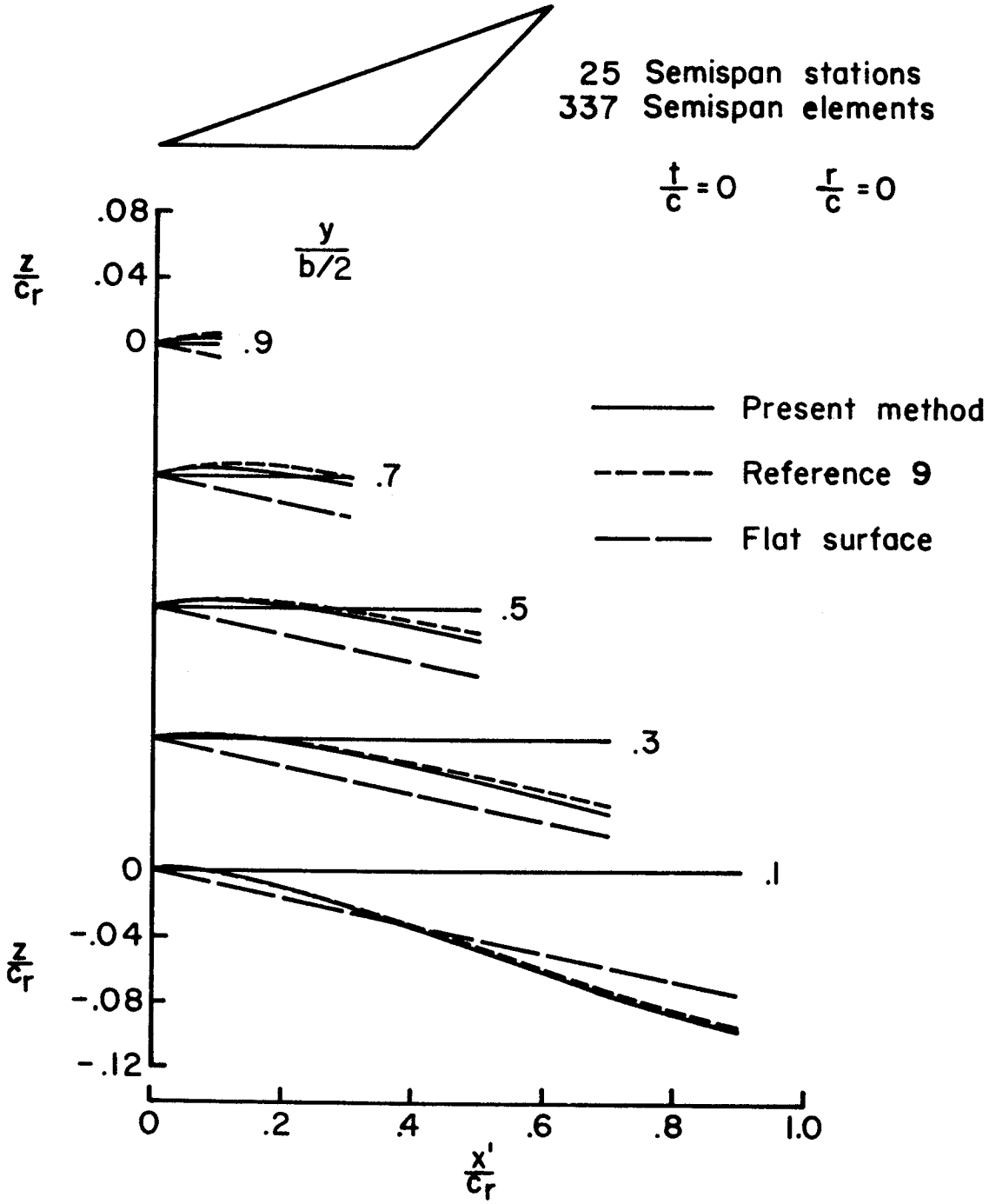

Figure 10.- Program geometric data for a 70° arrow wing camber surface design. M = 2.05, R = 0.0, $C_{L,des}$ = 0.16, no C_m restraint.

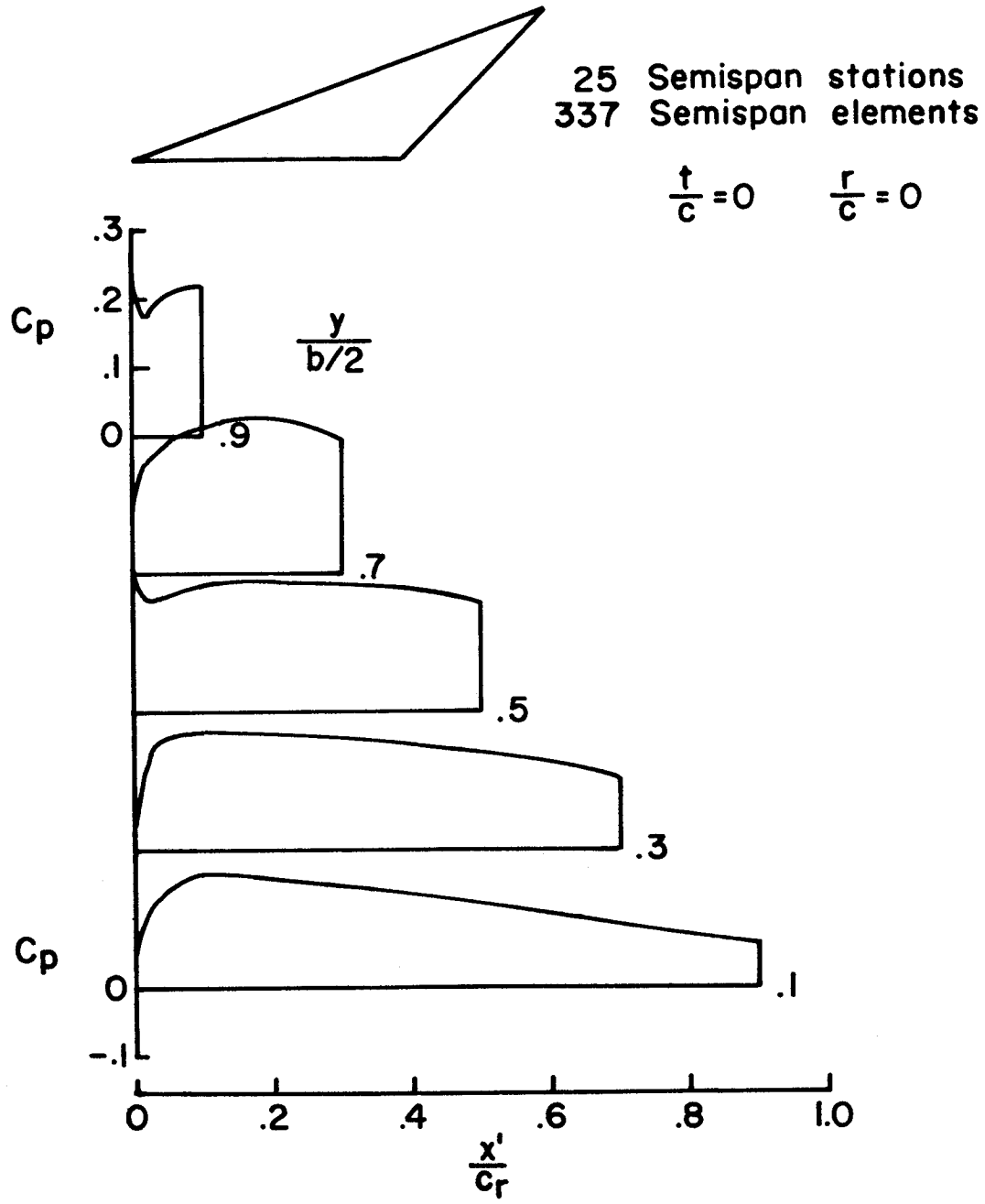

Figure 11.- Program pressure distribution for a 70° arrow wing camber surface design. M = 2.05, R = 0.0, $C_{L,des}$ = 0.16, no C_m restraint.

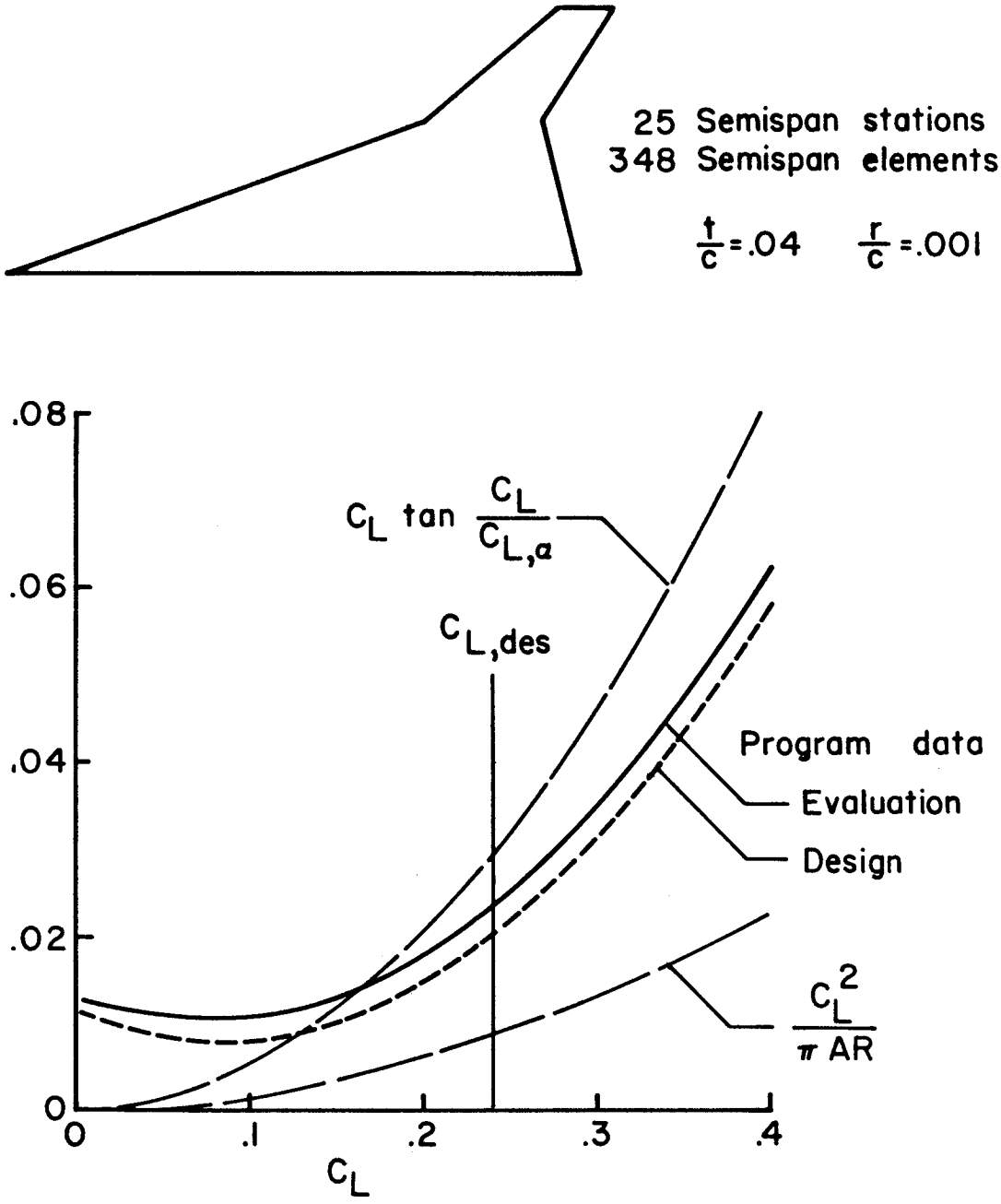

(a) Without adjustment of leading-edge surface factors.

Figure 12.- Program aerodynamic data for a supersonic fighter camber surface design. M = 2.0, R = 37 x 10^6, $C_{L,des}$ = 0.0.

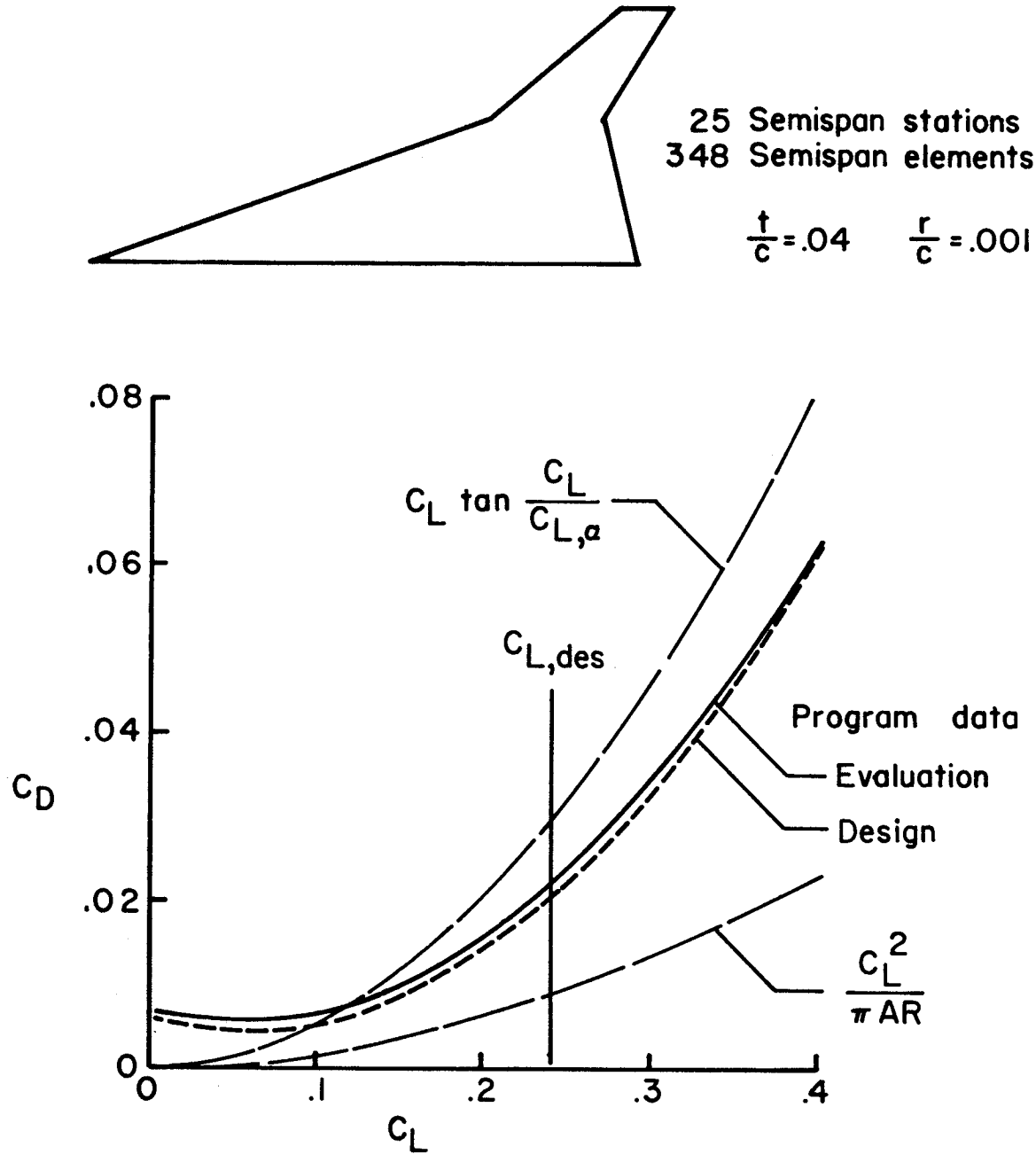

(b) With adjustment of leading-edge surface factors.

Figure 12.- Concluded.

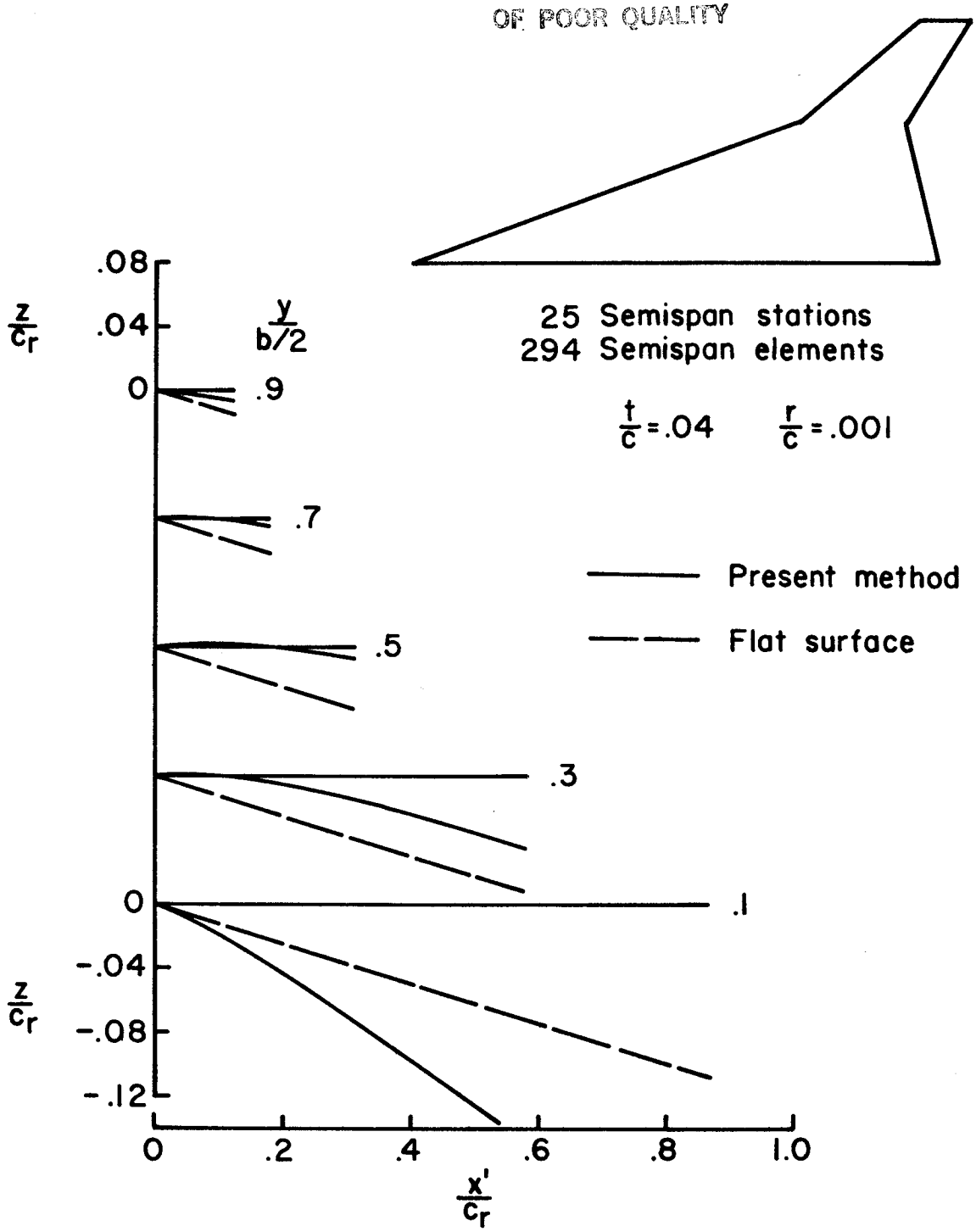

Figure 13.- Program geometric data for a supersonic fighter camber surface design. M = 2.0, R = 37 x 10^6, $C_{L,des}$ = 0.0.

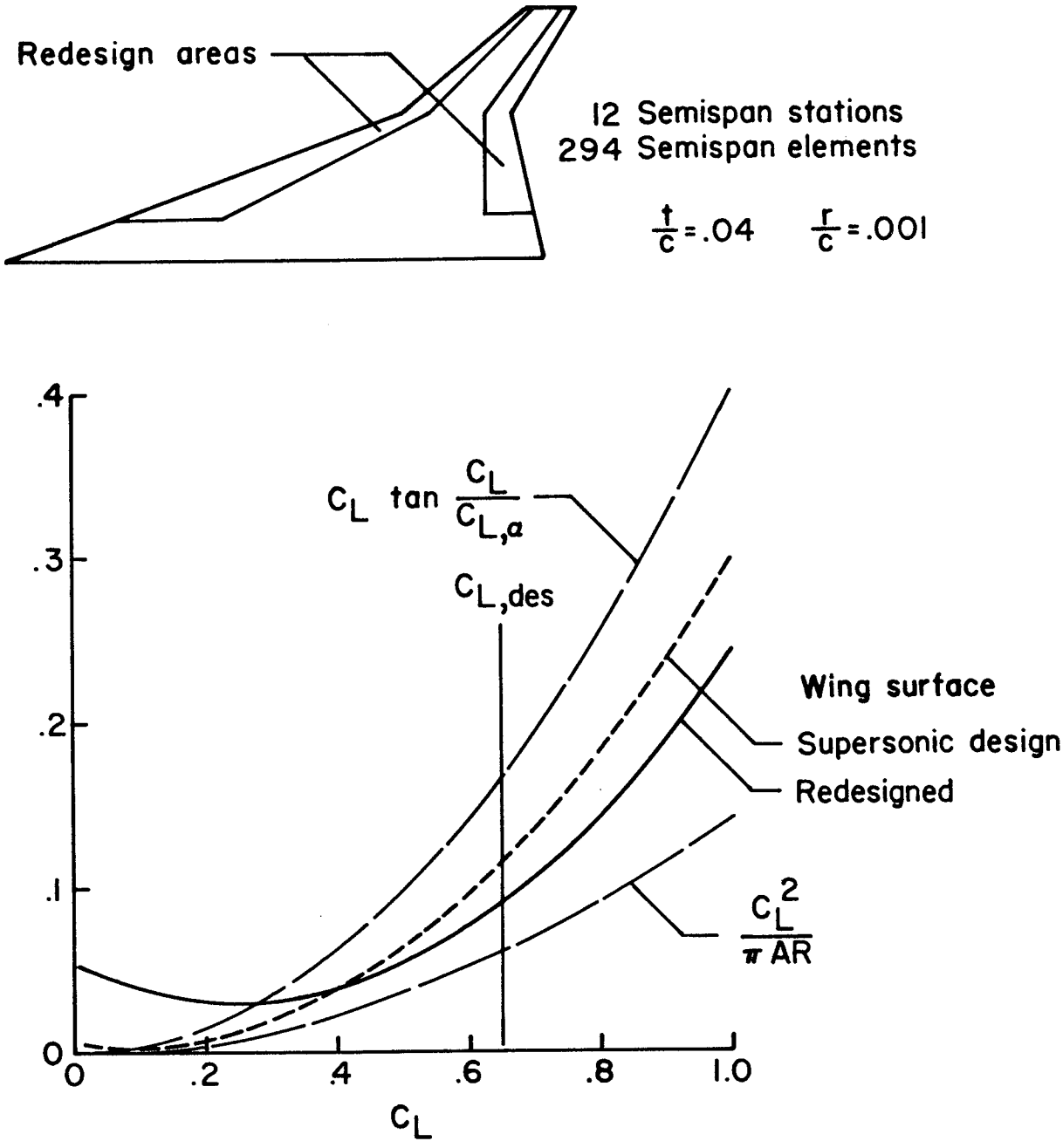

(a) Aerodynamic characteristics.

Figure 14.- Program evaluation data for a supersonic fighter camber surface with redesigned leading and trailing edges. M = 0.8, R = 52 x 10^6, $C_{L,des}$ = 0.65, $C_{m,des}$ = 0.0.

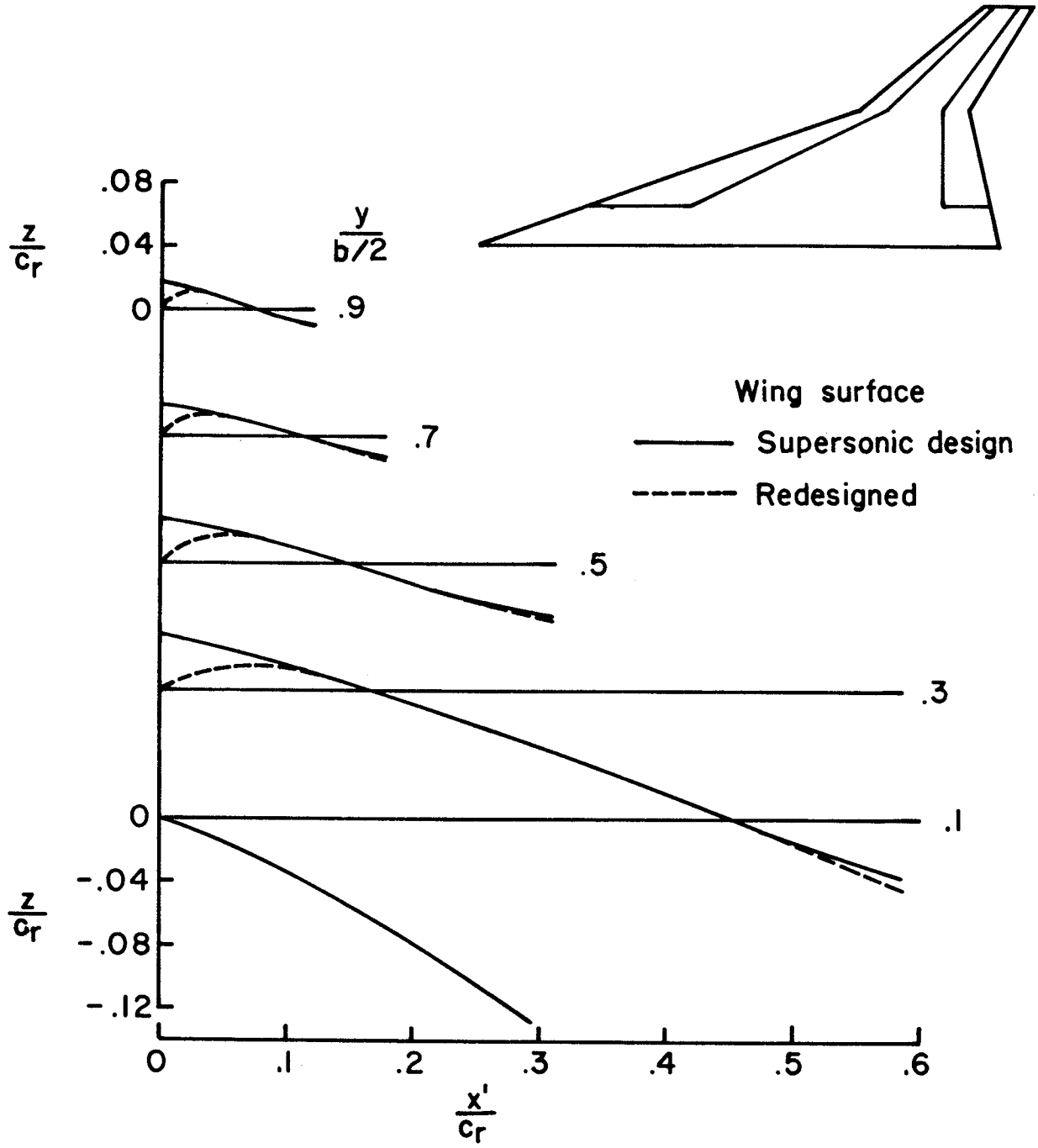

(b) Geometric characteristics.

Figure 14.- Concluded.

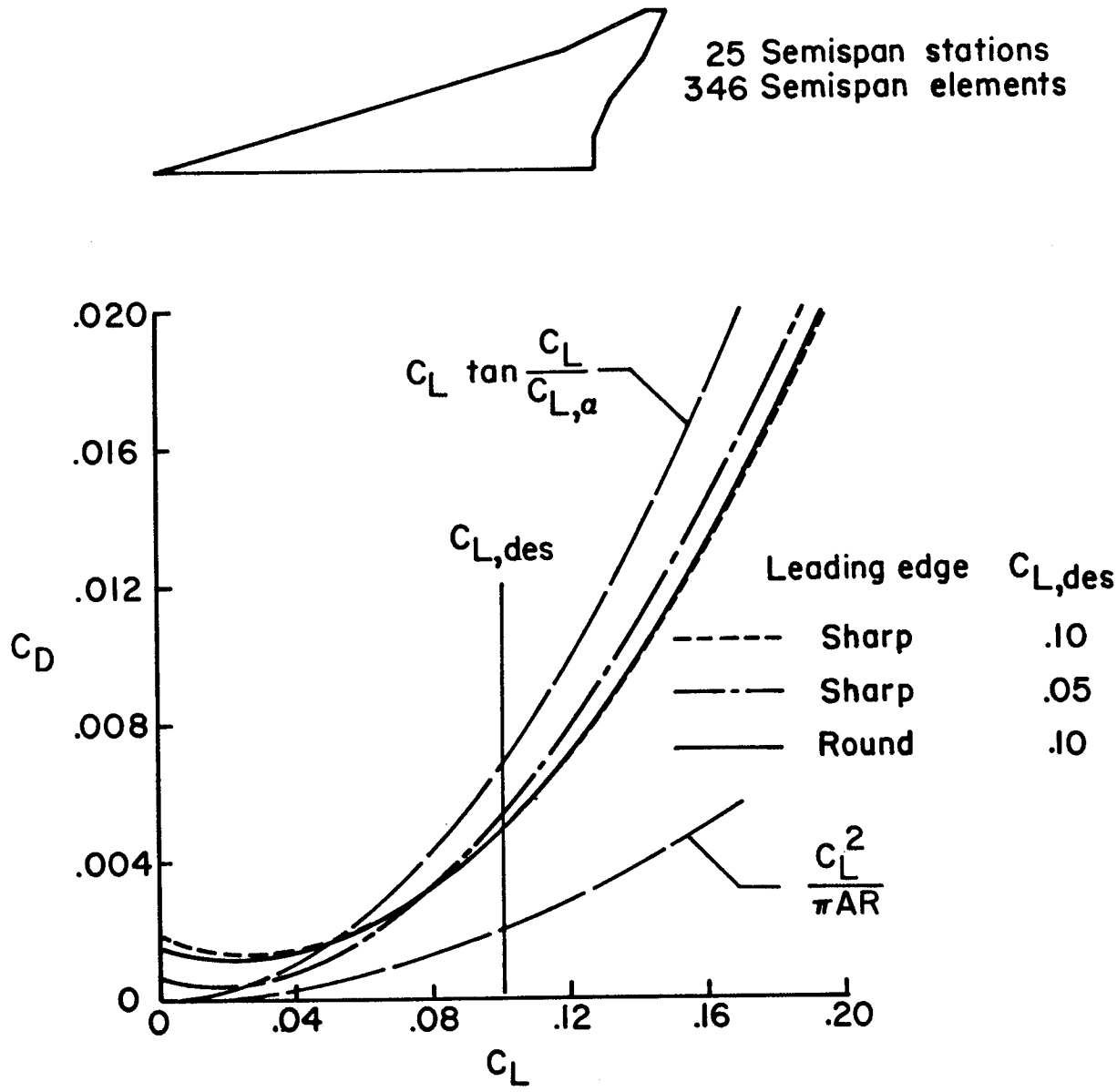

(a) Aerodynamic characteristics.

Figure 15.- Program evaluation data for supersonic transport camber surface designs with sharp and rounded leading edges. M = 2.7, R = 200.0 x 10^6, $C_{m,des}$ = 0.0.

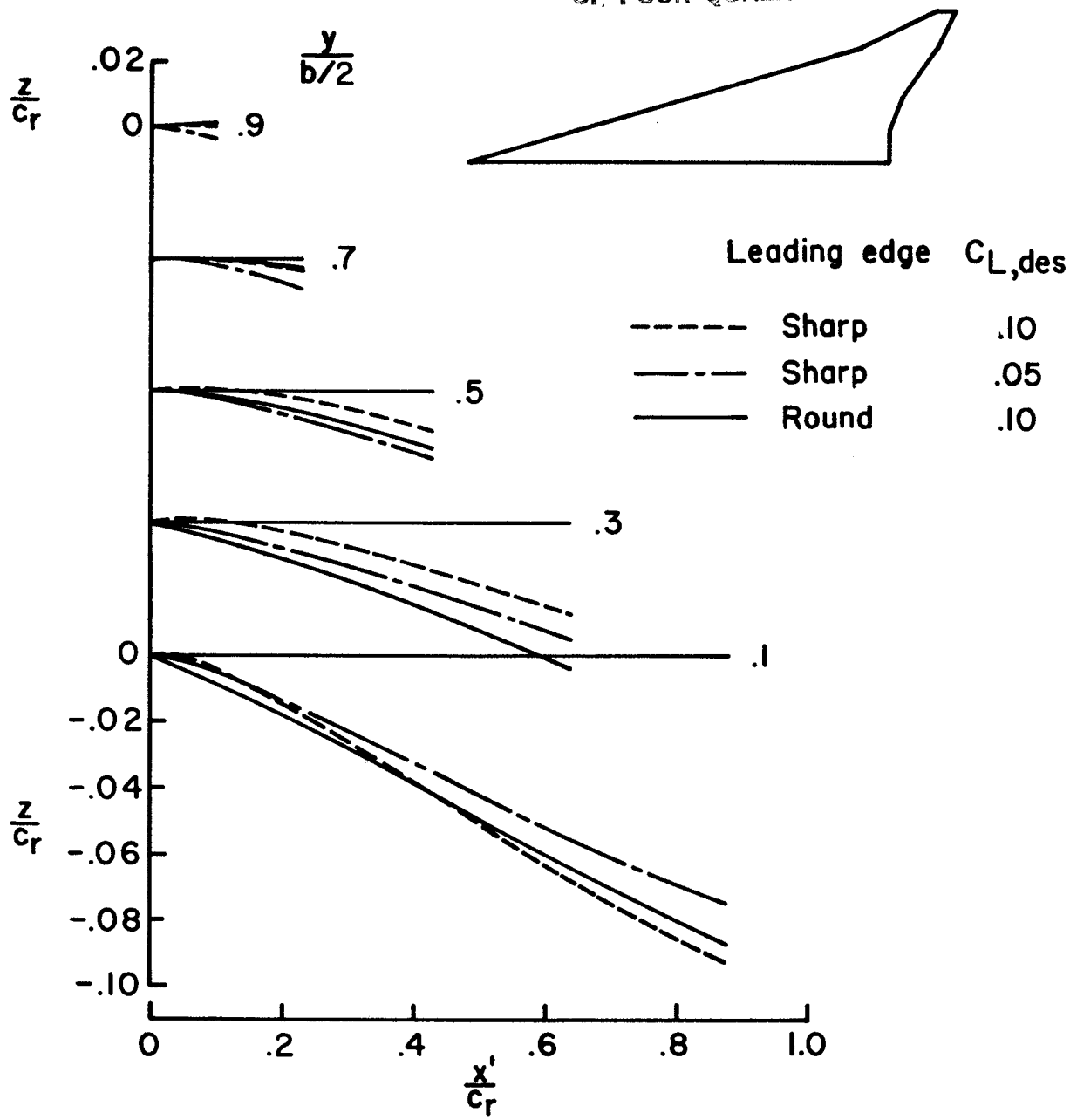

(b) Geometric characteristics.

Figure 15.- Concluded.

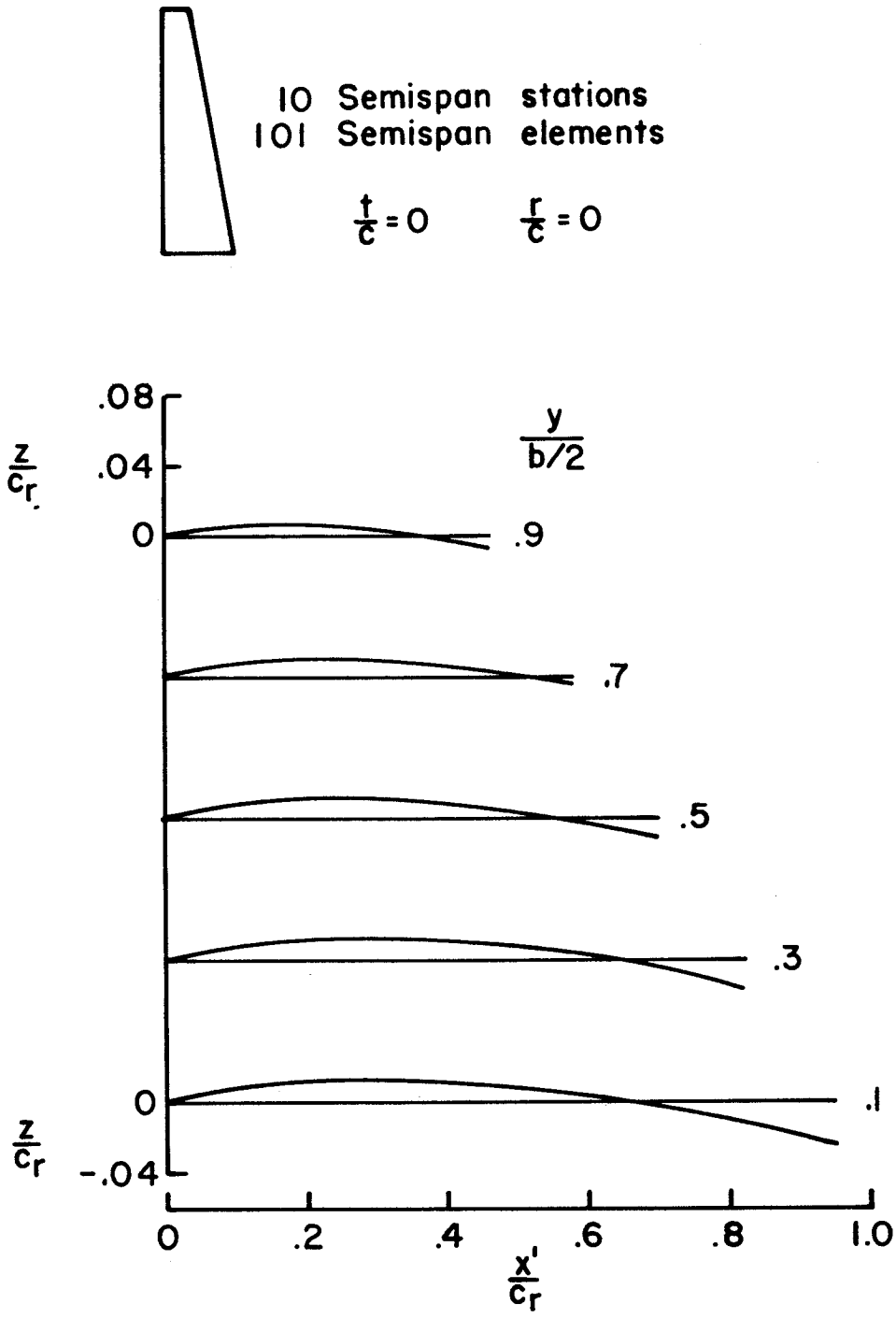

Figure 16.- Program geometric data for a general aviation wing camber surface design. M = 0.5, R = 0.0, $C_{L,des}$ = 0.35, no C_m restraint.

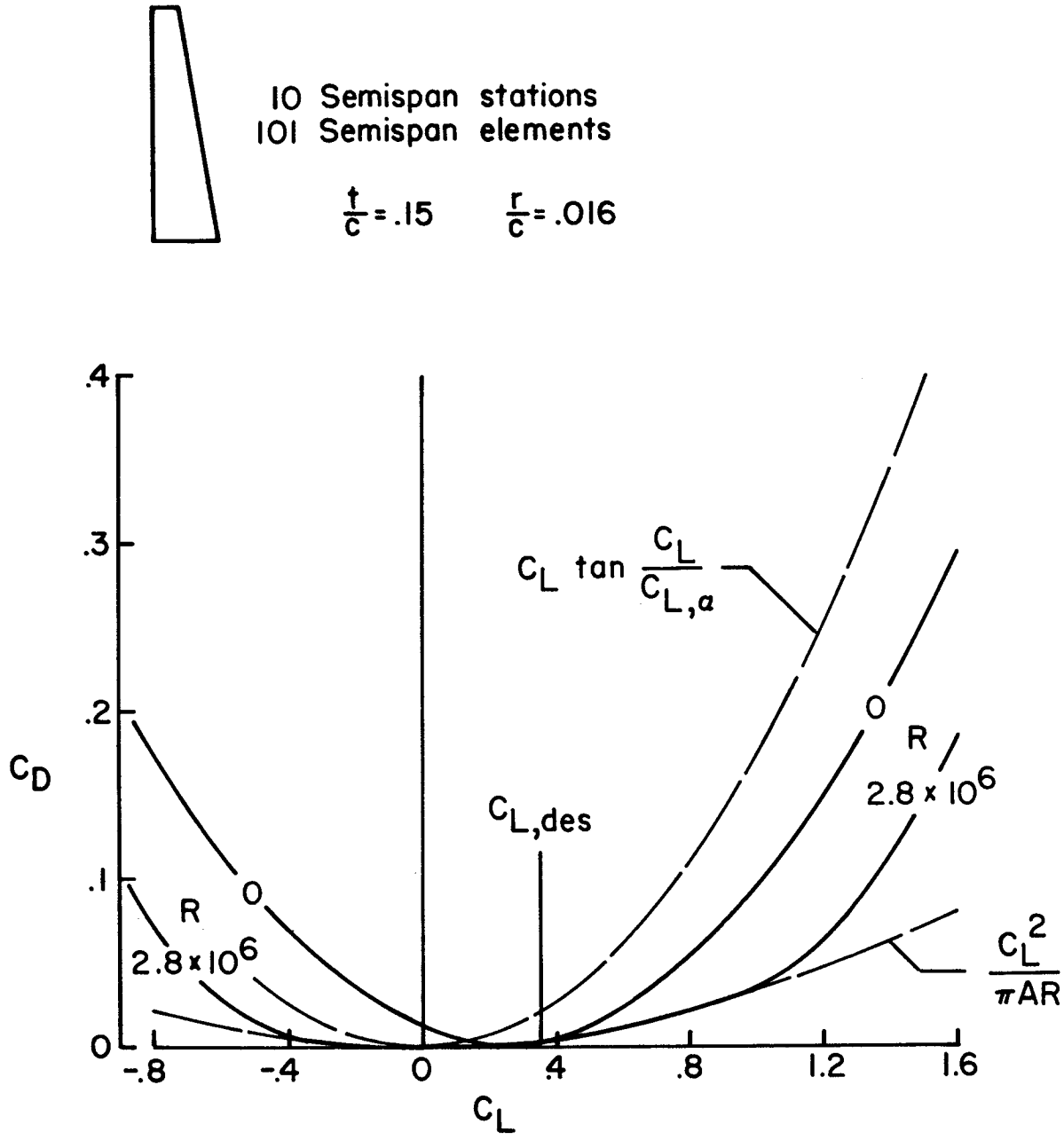

Figure 17.- Program aerodynamic evaluation data for a general aviation wing camber surface design. M = 0.5, R = 0.0, and 2.8 x 10^6.

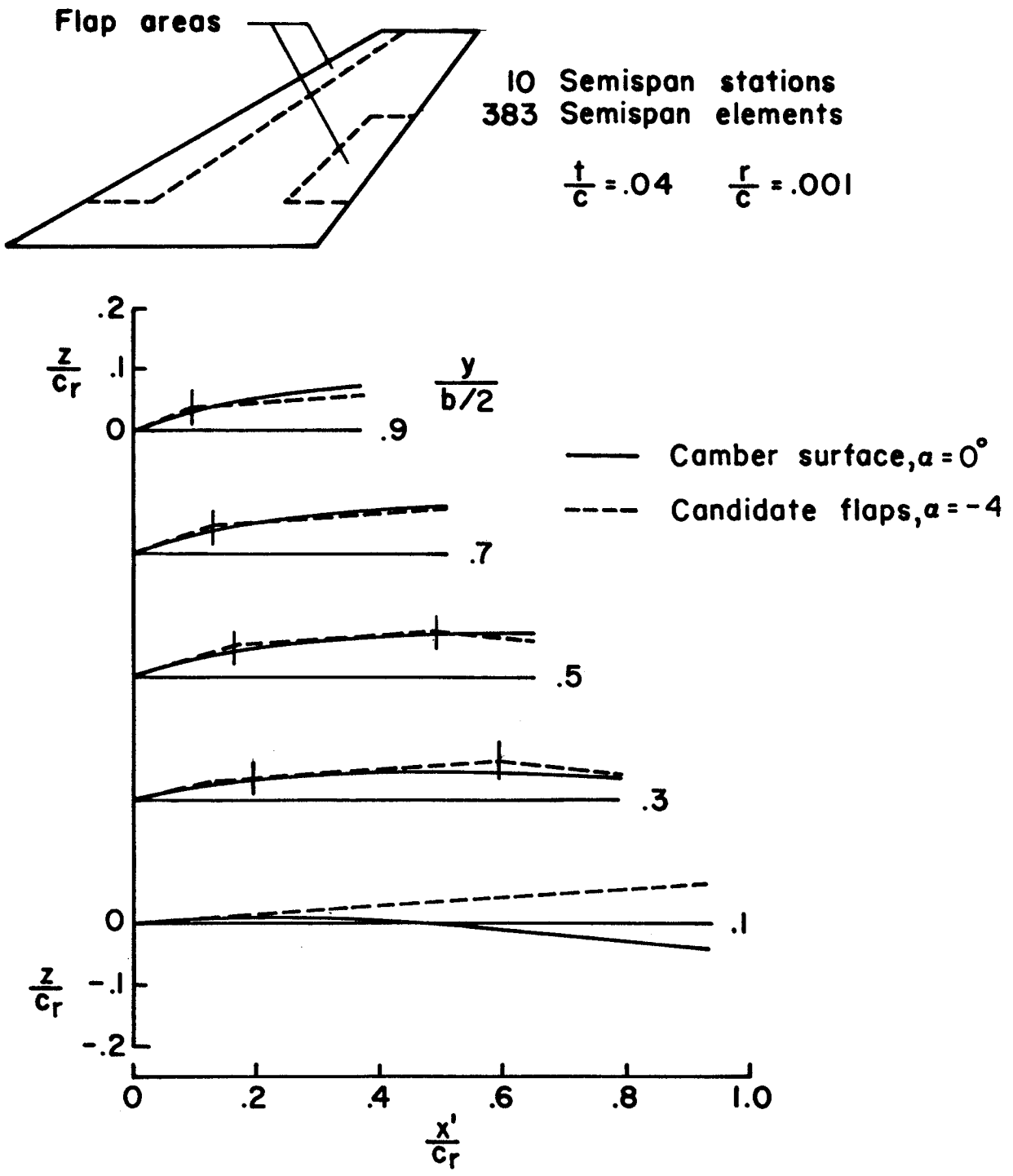

Figure 18.- An example of the use of the wing design program for the selection of candidate flap systems. M = 0.8, R = 50.0 x 10^6, $C_{L,des}$ = 0.5, no C_m restraint.

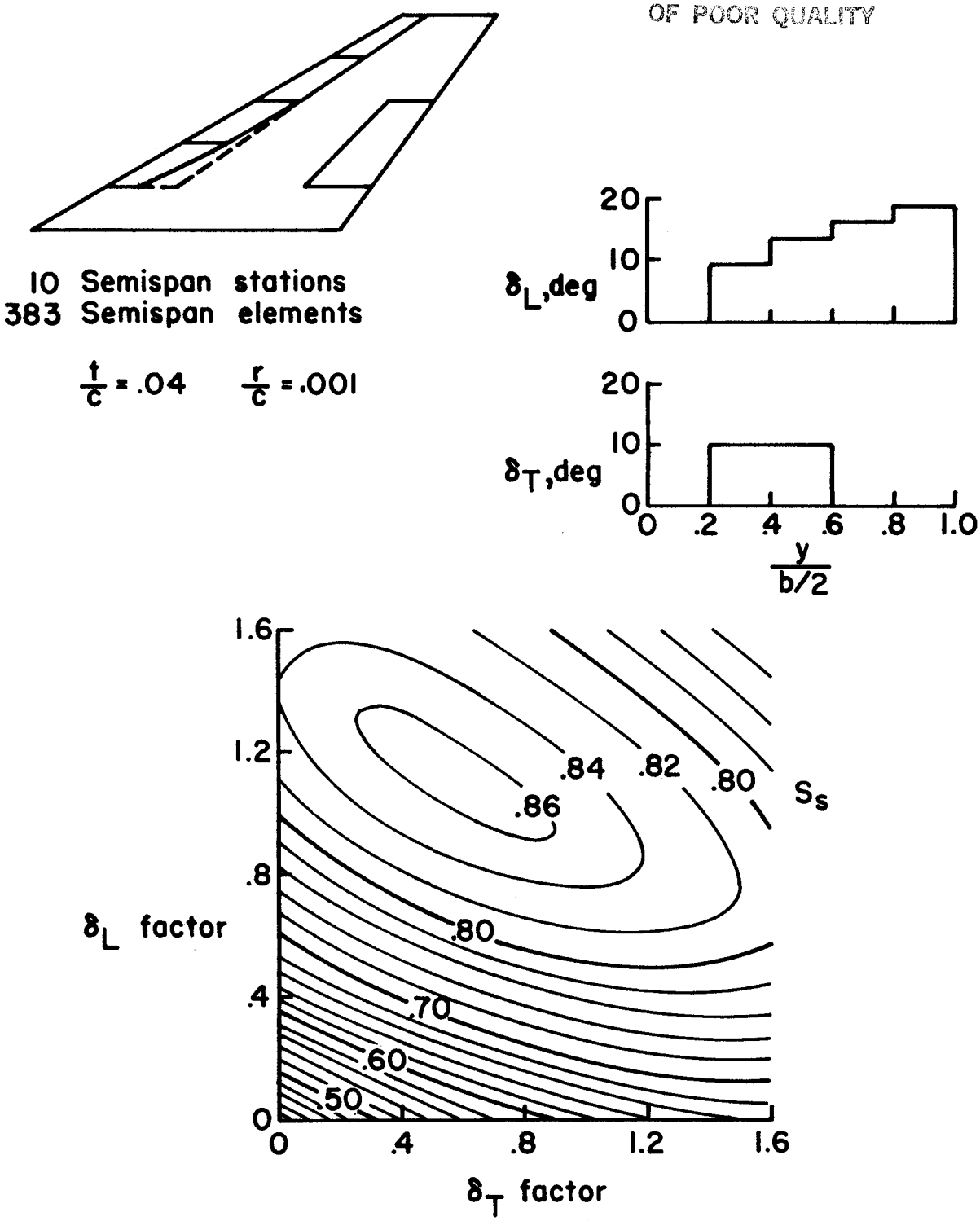

Figure 19.- Estimation of the aerodynamic performance of the candidate flap system as a function of deflection factors. M = 0.8, R = 50.0 x 10^6, C_L = 0.5.

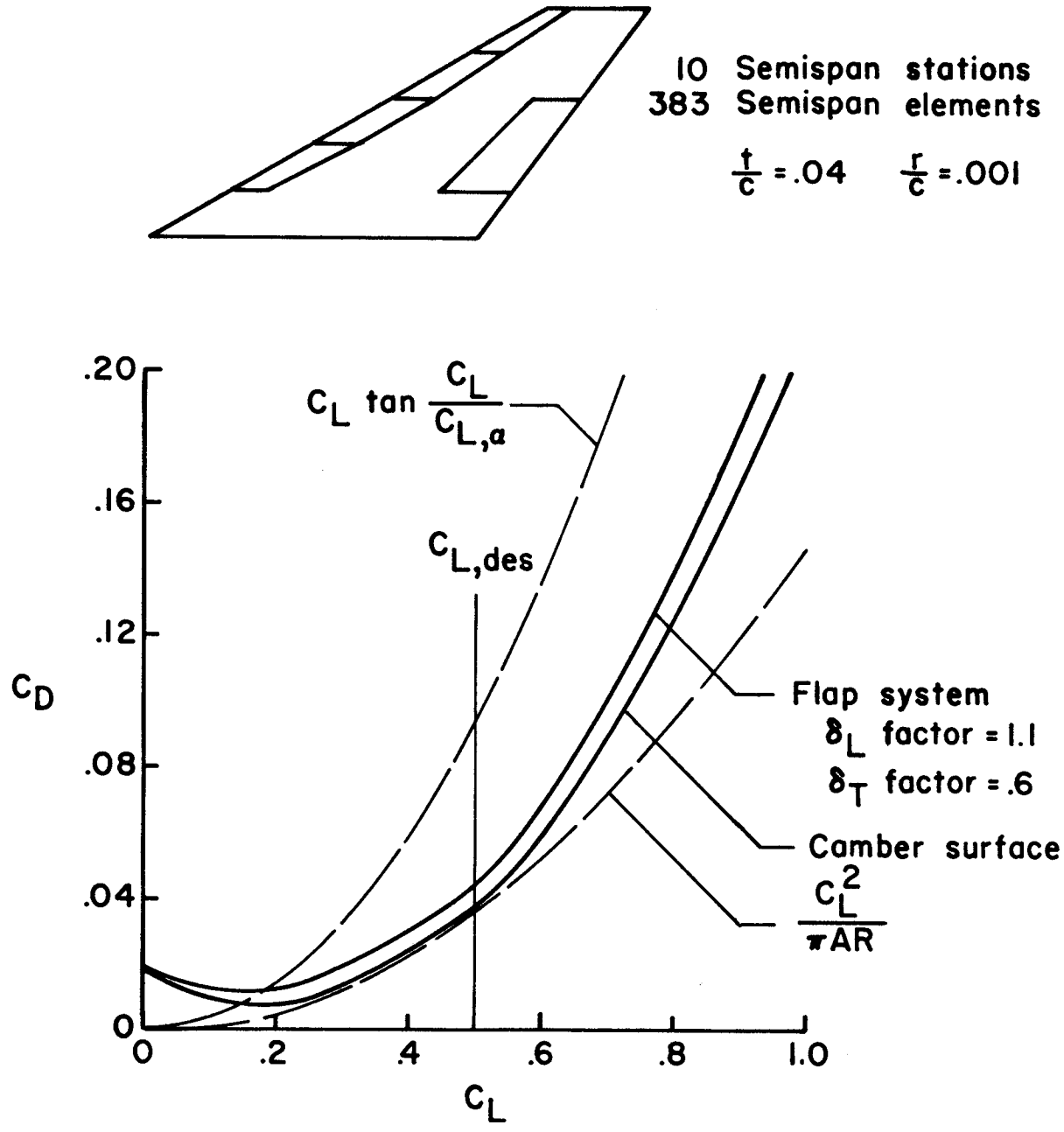

Figure 20.- Estimated aerodynamic characteristics for the best combination of leading and trailing edge flap deflection factors for the candidate flap system. M = 0.8, R =50 x 10^6.

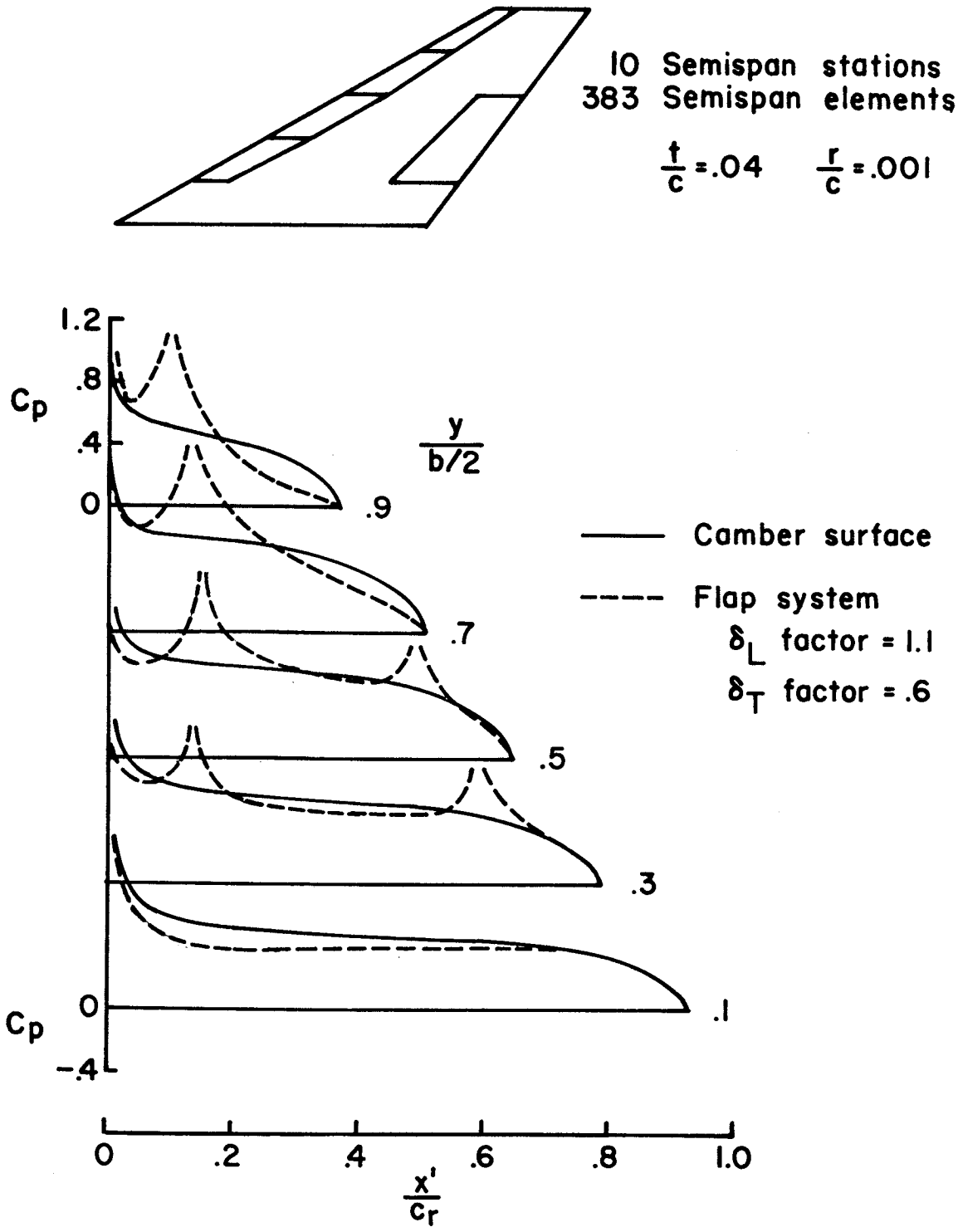

Figure 21.- Program pressure distributions for the flap system and the camber surface. M = 0.8, R =50 x 10^6, C_L = 0.5.

1. Report No.	2. Government Accession No.	3. Recipient's Catalog No.
NASA CR-3808		

4. Title and Subtitle	5. Report Date
NUMERICAL METHODS AND A COMPUTER PROGRAM FOR SUBSONIC AND SUPERSONIC AERODYNAMIC DESIGN AND ANALYSIS OF WINGS WITH ATTAINABLE THRUST CONSIDERATIONS	August 1984
	6. Performing Organization Code
7. Author(s)	8. Performing Organization Report No.
Harry W. Carlson and Kenneth B. Walkley	
	10. Work Unit No.
9. Performing Organization Name and Address	11. Contract or Grant No.
Kentron International Incorporated Hampton Technical Center Hampton, VA 23666	NAS1-16000
	13. Type of Report and Period Covered
12. Sponsoring Agency Name and Address	Contractor Report
National Aeronautics and Space Administration Washington, DC 20546	14. Sponsoring Agency Code 505-43-23-10

15. Supplementary Notes

Langley Technical Monitor: Christine M. Darden

16. Abstract

This paper describes methodology and an associated computer program for the design of wing lifting surfaces with attainable thrust taken into consideration. The approach is based on the determination of an optimum combination of a series of candidate surfaces rather than the more commonly used candidate loadings. Special leading-edge surfaces are selected to provide distributed leading-edge thrust forces which compensate for any failure to achieve the full theoretical leading-edge thrust, and a second series of general candidate surfaces is selected to minimize drag subject to constraints on the lift coefficient and, if desired, on the pitching moment coefficient. A primary purpose of the design approach is the introduction of attainable leading-edge thrust considerations so that relatively mild camber surfaces may be employed in the achievement of aerodynamic efficiencies comparable to those attainable if full theoretical leading-edge thrust could be achieved. The program provides an analysis as well as a design capability and is applicable to both subsonic and supersonic flow.

17. Key Words (Suggested by Author(s))	18. Distribution Statement
Aerodynamics Numerical methods Wing design Leading-edge thrust Linearized theory	[redacted]

19. Security Classif. (of this report)	20. Security Classif. (of this page)	21. No. of Pages	22. Price
Unclassified	Unclassified	77	